Table 2 Randomized trials of preoperative chemotherapy for esophageal cancers in Western countries.

Author	Year	Arm	Histology	*n*	MST (months)	OS	*P* value
Roth[28]	1988	CDDP/VDS/BLM + surgery + CDDP/VDS	SCC	19	9	25% (3-year)	
		Surgery alone		20	9	5% (3-year)	
Schlag[29]	1992	5-FU/CDDP + surgery	SCC	21	10	20% (1-year)	
		Surgery alone		24	10	32% (1-year)	
Nygaard[30]	1992	CDDP/BLM + surgery	SCC	56	7.5	6% (2-year)	
		Surgery alone		50	7.5	13% (2-year)	
Maipang[31]	1994	CDDP/VDS/BLM + surgery	SCC	24	17	31% (3-year)	
		Surgery alone		22	17	36% (3-year)	
Law[32]	1997	5-FU/CDDP + surgery	SCC	74	17	44% (2-year)	
		Surgery alone		73	13	31% (2-year)	0.17
Kelsen[33]	1998	5-FU/CDDP + surgery + 5-FU/CDDP	SCC/Adeno	213	15	23% (3-year)	
		Surgery alone		227	16	26% (3-year)	0.53
Ancona[34]	2001	5-FU/CDDP + surgery	SCC	48	25	41% (3-year)	
		Surgery alone		48	24	44% (3-year)	0.55
MRC[35]	2002	5-FU/CDDP + surgery	SCC/Adeno	400	17	43% (2-year)	
		Surgery alone		402	13	34% (2-year)	0.004

VDS, vindesine; BLM, bleomycin; SCC, squamous cell carcinoma; Adeno, adenocarcinoma; MST, median survival time; OS, overall survival rate; NA, not available

Systemic chemotherapy and surgery in Western countries

To date, two large randomized controlled studies have compared preoperative chemotherapy followed by surgery with surgery alone (Table 2).[28–35] In the U.S. intergroup trial (INT 113), 452 patients with adenocarcinomas or squamous cell carcinomas of the esophagus were randomly assigned to three cycles of 5-FU and cisplatin, followed by surgery, and additional postoperative chemotherapy, or surgery alone.[33] In this trial, there was no significant difference in overall survival or disease-free survival between perioperative chemotherapy and surgery alone. However, 19% of patients had an objective response to chemotherapy and those patients had a significantly better survival than those who had no objective response to chemotherapy or underwent surgery alone.

On the other hand, the UK Medical Research Council (MRC) trial showed survival benefits in preoperative chemotherapy.[35] In that trial, 802 patients with resectable esophageal cancers were randomized to two groups: patients who received two cycles of 5-FU and cisplatin followed by surgery or who underwent surgery alone. The curative resection (R0) rate was higher in the preoperative chemotherapy than the surgery alone group, although preoperative chemotherapy did not increase postoperative complications (R0 rate, 60% vs. 54%, $P < 0.0001$). Overall survival was significantly better in the preoperative chemotherapy group than surgery alone (2-year survival rate, 43% vs. 34%, $P = 0.004$). The median survival time (MST) was also improved in the preoperative chemotherapy group compared with surgery alone (MST, 16.8 vs. 13.3 months).

Several factors could have caused the conflicting results of the US intergroup trial and UK MRC trial. First, there were slight differences in dosage and duration of preoperative chemotherapy (three cycles in the US intergroup vs. two cycles in the MRC trial). The larger total dose of chemotherapy provided in the US intergroup may explain the difference in the number of patients proceeding to resection (80% in US intergroup vs. 92% in MRC trial). Second, the proportion of cases with adenocarcinoma in the MRC trial was 66%, which was slightly higher than the rate in the U.S. intergroup, at 54%. Third, the larger sample size of the MRC trial compared with the U.S. intergroup trial may readily allow detection of slight but clinically important differences in survival,.

In contrast to the conflicting results of the aforementioned large randomized controlled trials, a recent meta-analysis confirmed modest survival benefits of preoperative chemotherapy.[36] However, preoperative chemotherapy had no survival benefits in squamous cell carcinomas although the survival benefit was significant in adenocarcinomas. On the other hand, the meta-analysis showed a significant survival benefit for preoperative chemoradiation, irrespective of whether the histopathological type was squamous cell carcinoma or adenocarcinoma. This finding prompted the question of whether preoperative chemotherapy is superior to chemoradiotherapy. Only one study has compared

preoperative chemotherapy with preoperative chemoradiotherapy.[37] In that trial, 126 patients with locally advanced (T3-4NXM0) adenocarcinoma of the lower esophagus or gastric cardia were randomly allocated to one of two treatment groups: the chemotherapy group [2.5 courses of preoperative chemotherapy (cisplatin, 5-FU, and leucovorin) followed by surgery] and the chemoradiotherapy group [2 courses of the same chemotherapy followed by chemoradiotherapy (30 Gy), then surgery]. The rate of pathological complete response (pCR) was significantly higher in the preoperative chemoradiotherapy group than in the preoperative chemotherapy group (15.6% vs. 2%, $P = 0.03$), although there was no significant difference in the rate of curative resection between the two groups. Preoperative chemoradiotherapy tended to be associated with a better prognosis than preoperative chemotherapy, although this difference did not reach statistical significance because of early closure and the small sample size of this trial (3-year survival rate, 47.4% vs. 27.7%, $P = 0.07$). Based on the results of these trials, preoperative chemoradiotherapy followed by surgery has been become the standard treatment strategy in Western counties for potentially resectable esophageal cancers.

Future directions

At present, chemotherapy consisting of 5-FU and cisplatin is accepted as the standard chemotherapy for esophageal cancers. However, the reported response rate to this chemotherapy for esophageal cancers remains at a 30–40% level.[38,39] Previous studies that assessed the effectiveness of preoperative chemotherapy demonstrated a better survival of clinical responders.[33,34,40] Thus, to improve the overall prognosis of patients who undergo preoperative chemotherapy followed by surgery, we need to explore new preoperative chemotherapeutic regimens that yield response rates higher than that of the conventional chemotherapy of 5-FU and cisplatin. One of the most promising chemotherapeutic regimens is the combination of 5-FU, cisplatin, and docetaxel. A gastric cancer TAX325 study, in which 445 patients with advanced gastric cancers were randomly assigned and treated with either docetaxel plus cisplatin and 5-FU (DCF) or cisplatin and 5-FU (CF), demonstrated that DCF is superior to CF with regard to progression-free survival and overall survival as well as the overall response rate.[41] Including patients with advanced head and neck cancers, two recent large randomized trials (TAX323, TAX324) compared induction chemotherapy using docetaxel plus cisplatin and 5-FU or cisplatin and 5-FU, followed by chemoradiotherapy or radiotherapy. Both studies demonstrated that the addition of docetaxel significantly improved progression-free and overall survival, compared with the standard regimen of cisplatin and 5-FU.[42,43] Thus, in head and neck cancer and gastric cancer, the superiority of chemotherapy of docetaxel/cisplatin/5-FU to the standard 5-FU/cisplatin has been established. In Japan, a phase I/II study (JCOG0807), designed to evaluate the effectiveness of chemotherapy of docetaxel/cisplatin/5-FU, is currently being conducted in patients with inoperable and/or recurrent esophageal cancers.

In addition to this, TS-1 is a potentially promising chemotherapeutic agent for esophageal cancers. TS-1 has been widely used in various cancers, such as head and neck cancer, lung cancer, and pancreatic cancer, and the combination chemotherapy of TS-1 plus cisplatin has been established as the standard chemotherapeutic regimen in gastric cancer. In esophageal cancers, the JCOG0604 study is currently being conducted to evaluate the effectiveness of definitive chemoradiotherapy consisting TS-1 plus cisplatin and 50.4-Gy radiotherapy in patients with clinical stage II/III esophageal cancers. In addition to TS-1, molecular target therapy agents for various cancers have been attracting much attraction recently. A recent study showed that cetuximab, an epidermal growth factor receptor (EGFR) antibody, improved prognosis of patients with advanced head and neck cancer who received concurrent radiotherapy.[44] In esophageal cancers, the addition of cetuximab to cisplatin and 5-FU with or without radiotherapy has been examined in recent trials, and the results are encouraging for cetuximab.[45,46] Studies of molecular target agents for esophageal cancers have just begun, and the clinical application of molecular target agents including cetuximab to systemic chemotherapy for esophageal cancers will be expected in the future.

Finally, in Japan, preoperative chemotherapy followed by surgery has been recognized as the standard treatment strategy for patients with resectable esophageal cancers. On the other hand, in Western countries, preoperative chemoradiotherapy followed by surgery is widely applied in patients with advanced esophageal cancers. Even after allowing for the difference in the dominant histopathological type and operative procedures between the two patient populations, there is a need to examine in the near future which of the treatment strategies is more effective in patients with resectable esophageal cancers.

References

1. Altorki N, Skinner D. Should en bloc esophagectomy be the standard care for esophageal carcinoma? Ann Surg 2001;234:581–7.

2. Akiyama H, Tsurumaru M, Udagawa H, Kajiyama Y. Radical lymph node dissection for cancer of the thoracic esophagus. Ann Surg 1994;220:364–72.
3. Dresner SM, Griffin SM. Pattern of recurrence following radical oesophagectomy with two field lymphadenectomy. Br J Surg 2000;87:1426–33.
4. Nakagawa S, Kanda T, Kosugi S, Ohashi M, Suzuki T, Hatakeyama K. Recurrence pattern of squamous cell carcinoma of the thoracic esophagus after extended radical esophagectomy with three-field lymphadenectomy. J Am Coll Surg 2004;198:205–11.
5. Hulscher JB, van Sandick JW, Tijssen JG, Obertop H, van Lanschot JJ. The recurrence pattern of esophageal carcinoma after transhiatal resection. J Am Coll Surg 2000;191:143–8.
6. Bhansali MS, Fujita H, Kakegawa T, Yamana H, Ono T, Hikita S, et al. Pattern of recurrence after extended radical esophagectomy with three-field lymph node dissection for squamous cell carcinoma in the thoracic esophagus. World J Surg 1997;21:275–81.
7. Chen G, Wang Z, Liu XY, Liu FY. Recurrence pattern of squamous cell carcinoma in the middle thoracic esophagus after modified Ivor–Lewis esophagectomy. World J Surg 2007;31:1107–4.
8. Mariette C, Balon JM, Piessen G, Fabre S, Van Seuningen I, Triboulet JP. Pattern of recurrence following complete resection of esophageal carcinoma and factors predictive of recurrent disease. Cancer (Phila) 2003;97:1616–23.
9. Kato H, Watanabe H, Tachimori Y, et al. Evaluation of neck lymph node dissection for thoracic esophageal carcinoma. Ann Thorac Surg 1991;51:931–5.
10. Isono K, Sato H, Nakayama K. Results of a nationwide study on the three-field lymph node dissection of esophageal cancer. Oncology 1991;48:411–20.
11. Nishihira T, Hirayama K, Mori S. A prospective randomized trial of extended cervical and superior mediastinal lymphadenectomy for carcinoma of the thoracic esophagus. Am J Surg 1998;175:47–51.
12. Fujita H, Sueyoshi S, Tanaka T, Fujii T, Toh U, Mine T, et al. Optimal lymphadenectomy for squamous cell carcinoma in the thoracic esophagus: comparing the short- and long-term outcome among the four types of lymphadenectomy. World J Surg 2003;27:571–9.
13. Walsh TN, Noonan N, Hollywood D, Kelly A, Keeling N, Hennessy TP. A comparison of multimodal therapy and surgery for esophageal adenocarcinoma. N Engl J Med 1996;335:462–7.
14. Tepper J, Krasna MJ, Niedzwiecki D, Hollis D, Reed CE, Goldberg R, et al. Phase III trial of trimodality therapy with cisplatin, fluorouracil, radiotherapy, and surgery compared with surgery alone for esophageal cancer: CALGB 9781. J Clin Oncol 2008;26:1086–92.
15. Bosset JF, Gignoux M, Triboulet JP, Tiret E, Mantion G, Elias D, et al. Chemoradiotherapy followed by surgery compared with surgery alone in squamous-cell cancer of the esophagus. N Engl J Med 1997;337:161–7.
16. Urba S, Orringer M, Turrisi A, Iannettoni M, Forastiere A, Strawderman M. A randomized trial comparing surgery (S) to preoperative concomitant chemoradiation plus surgery in patients (pts) with respectable esophageal cancer (CA): updated analysis. Proc Am Soc Clin Oncol 1997;16:A983.
17. Nyggard K, Hagen S, Hansen H S, Hatlevoll R, Hultbom R, Jakobsen A, et al. Pre-operative radiotherapy prolongs survival in operable esophageal carcinoma: a randomized, multicenter study of pre-operative radiotherapy and chemotherapy. The second Scandinavian trial in esophageal cancer. World J Surg 1992;16:1104–10.
18. Le Prise E, Etienne PL, Meunier B, Maddem G, Ben Hassel M, Gedouin D, et al. A randomized study of chemotherapy, radiation therapy, and surgery versus surgery for localized squamous cell carcinoma of the esophagus. Cancer (Phila) 1994;73:1779–84.
19. Apinop C, Puttisak P, Preecha N. A prospective study of combined therapy in esophageal cancer. Hepatogastroenterology 1994;41:391–3.
20. Burmeister BH, Smithers BM, Gebski V, Fitzgerald L, Simes RJ, Devitt P, et al. Surgery alone versus chemoradiotherapy followed by surgery for resectable cancer of the oesophagus: a randomised controlled phase III trial. Lancet Oncol 2005;6:659–68.
21. Brown LM, Devesa SS, Chow WH. Incidence of adenocarcinoma of the esophagus among white Americans by sex, stage, and age. J Natl Cancer Inst 2008;100:1184–7.
22. Holmes RS, Vaughan TL. Epidemiology and pathogenesis of esophageal cancer. Semin Radiat Oncol 2007;17:2–9.
23. Ando N, Ozawa S, Kitagawa Y, Shinozawa Y, Kitajima M. Improvement in the results of surgical treatment of advanced squamous esophageal carcinoma during 15 consecutive years. Ann Surg 2000;232:225–32.
24. Ando N, Iizuka T, Kakegawa T, Isono K, Watanabe H, Ide H, et al. A randomized trial of surgery with and without chemotherapy for localized squamous carcinoma of the thoracic esophagus: the Japan Clinical Oncology Group Study. J Thorac Cardiovasc Surg 1997;114:205–9.
25. Ando N, Iizuka T, Ide H, Ishida K, Shinoda M, Nishimaki T, et al. Surgery plus chemotherapy compared with surgery alone for localized squamous cell carcinoma of the thoracic esophagus: a Japan Clinical Oncology Group Study–JCOG9204. J Clin Oncol 2003;21:4592–6.
26. Igaki H, Kato H, Ando N, Shinoda M, Shimizu H, Nakamura T, et al. A randomized trial of postoperative adjuvant chemotherapy with cisplatin and 5-fluorouracil versus neoadjuvant chemotherapy for clinical stage II/III squamous cell carcinoma of the thoracic esophagus (JCOG9907). J Clin Oncol 2008;26(suppl):215s (abstract 4510).
27. Kato K, Muro K, Minashi K, Ohtsu A, Ishikura S, Boku N, et al. Phase II study of chemoradiotherapy with 5-fluorouracil and cisplatin for stage II–III esophageal squamous cell carcinoma: JCOG Trial (JCOG 9906). Int J Radiat Oncol Biol Phys 2010: [Epub ahead of print].
28. Roth JA, Pass HI, Flanagan MM, Graeber GM, Rosenberg JC, Steinberg S. Randomized clinical trial of preoperative and postoperative adjuvant chemotherapy with cisplatin, vindesine, and bleomycin for carcinoma of the esophagus. J Thorac Cardiovasc Surg 1988;96:242–8.
29. Schlag PM. Randomized trial of preoperative chemotherapy for squamous cell cancer of the esophagus. The Chirurgische Arbeitsgemeinschaft Fuer Onkologie der Deutschen Gesellschaft Fuer Chirurgie Study Group. Arch Surg 1992;127:1446–50.
30. Nygaard K, Hagen S, Hansen HS, Hatlevoll R, Hultborn R, Jakobsen A, et al. Pre-operative radiotherapy prolongs survival in operable esophageal carcinoma: a randomized, multicenter study of pre-operative radiotherapy and chemotherapy. The second Scandinavian trial in esophageal cancer. World J Surg 1992;16:1104–9.
31. Maipang T, Vasinanukorn P, Petpichetchian C, Chamroonkul S, Geater A, Chansawwaang S, et al. Induction chemotherapy in the treatment of patients with carcinoma of the esophagus. J Surg Oncol 1994;56:191–7.
32. Law S, Fok M, Chow S, Chu KM, Wong J. Preoperative chemotherapy versus surgical therapy alone for squamous cell carcinoma of the esophagus: a prospective randomized trial. J Thorac Cardiovasc Surg 1997;114:210–7.

33. Kelsen DP, Ginsberg R, Pajak TF, Sheahan DG, Gunderson L, Mortimer J, et al. Chemotherapy followed by surgery compared with surgery alone for localized esophageal cancer. N Engl J Med 1998;339:1979–84.
34. Ancona E, Ruol A, Santi S, Merigliano S, Sileni VC, Koussis H, et al. Only pathologic complete response to neoadjuvant chemotherapy improves significantly the long-term survival of patients with respectable esophageal squamous cell carcinoma. Cancer (Phila) 2001;91:2165–74.
35. Medical Research Council Oesophageal Cancer Working Group. Surgical resection with or without preoperative chemotherapy in oesophageal cancer: a randomized controlled trial. Lancet 2002;359:1727–33.
36. Gebski V, Burmeister B, Smithers BM, Foo K, Zalcberg J, Simes J, et al. Survival benefits from neoadjuvant chemoradiotherapy or chemotherapy in oesophageal carcinoma: a meta-analysis. Lancet Oncol 2007;8:226–34.
37. Stahl M, Walz MK, Stuschke M, Lehmann N, Meyer HJ, Riera-Knorrenschild J, et al. Phase III comparison of preoperative chemotherapy compared with chemoradiotherapy in patients with locally advanced adenocarcinoma of the esophagogastric junction. J Clin Oncol 2009;27:851–6.
38. Iizuka T, Kakegawa T, Ide H, Ando N, Watanabe H, Tanaka O, et al. Phase II evaluation of cisplatin and 5-fluorouracil in advanced squamous cell carcinoma of the esophagus: a Japanese Esophageal Oncology Group Trial. Jpn J Clin Oncol 1992;22:172–6.
39. Hayashi K, Ando N, Watanabe H, Ide H, Nagai K, Aoyama N, et al. Phase II evaluation of protracted infusion of cisplatin and 5-fluorouracil in advanced squamous cell carcinoma of the esophagus: a Japan Esophageal Oncology Group (JEOG) Trial (JCOG9407). Jpn J Clin Oncol 2001;31:419–23.
40. Miyata H, Yoshioka A, Yamasaki M, Nushijima Y, Takiguchi S, Fujiwara Y, et al. Tumor budding in tumor invasive front predicts prognosis and survival of patients with esophageal squamous cell carcinomas receiving neoadjuvant chemotherapy. Cancer (Phila) 2009;115:3324–34.
41. Van Cutsem E, Moiseyenko VM, Tjulandin S, Majlis A, Constenla M, Boni C, et al. Phase III study of docetaxel and cisplatin plus fluorouracil compared with cisplatin and fluorouracil as first-line therapy for advanced gastric cancer: a report of the V325 Study Group. J Clin Oncol 2006;24:4991–7.
42. Vermorken JB, Remenar E, van Herpen C, Gorlia T, Mesia R, Degardin M, et al. Cisplatin, fluorouracil, and docetaxel in unresectable head and neck cancer. N Engl J Med 2007;357:1695–704.
43. Posner MR, Hershock DM, Blajman CR, Mickiewicz E, Winquist E, Gorbounova V, et al. Cisplatin and fluorouracil alone or with docetaxel in head and neck cancer. N Engl J Med 2007;357:1705–15.
44. Bonner JA, Harari PM, Giralt J, Azarnia N, Shin DM, Cohen RB, et al. Radiotherapy plus cetuximab for squamous cell carcinoma of the head and neck. N Engl J Med 2006;354:567–8.
45. Safran H, Suntharalingam M, Dipetrillo T, Ng T, Doyle LA, Krasna M, et al. Cetuximab with concurrent chemoradiation for esophageal cancer: assessment of toxicity. Int J Radiat Oncol Biol Phys 2008;70:391–5.
46. Lorenzen S, Schuster T, Porschen R, et al. Cetuximab plus cisplatin-5-fluorouracil versus cisplatin-5-fluorouracial alone in first-line metastatic squamous cell carcinoma of the esophagus: a randomized phase II study of the Arbeitsgemeinschaft Internistische Onkologie. Ann Oncol 2009;20:1667–73.

Leukemia (2011) 25, 1849–1856

www.nature.com/leu

ORIGINAL ARTICLE

Eμ/miR-125b transgenic mice develop lethal B-cell malignancies

Y Enomoto[1], J Kitaura[1], K Hatakeyama[2], J Watanuki[3], T Akasaka[4], N Kato[1], M Shimanuki[3], K Nishimura[1], M Takahashi[1], M Taniwaki[5], C Haferlach[6], R Siebert[7], MJS Dyer[4], N Asou[8], H Aburatani[9], H Nakakuma[3], T Kitamura[1,10] and T Sonoki[3]

[1]*Division of Cellular Therapy, The Institute of Medical Science, The University of Tokyo, Tokyo, Japan;* [2]*Department of Pathology, Faculty of Medicine, University of Miyazaki, Miyazaki, Japan;* [3]*Hematology/Oncology, Wakayama Medical University, Wakayama, Japan;* [4]*MRC Toxicology Unit/University of Leicester, Leicester, UK;* [5]*Division of Hematology and Oncology, Department of Medicine, Kyoto Prefectural University of Medicine, Kyoto, Japan;* [6]*MLL Münchner Leukämielabor GmbH Max-Lebsche-Platz, München, Germany;* [7]*Institute of Human Genetics, Christian-Albrechts-University Kiel/University Hospital Schleswig-Holstein, Kiel, Germany;* [8]*Department of Hematology, Kumamoto University School of Medicine, Kumamoto, Japan;* [9]*Genome Science Division, Research Center for Advanced Science and Technology, The University of Tokyo, Tokyo, Japan and* [10]*Division of Stem Cell Signaling, The Institute of Medical Science, The University of Tokyo, Tokyo, Japan*

***MicroRNA-125b-1 (miR-125b-1)* is a target of a chromosomal translocation t(11;14)(q24;q32) recurrently found in human B-cell precursor acute lymphoblastic leukemia (BCP-ALL). This translocation results in overexpression of miR-125b controlled by immunoglobulin heavy chain gene (*IGH*) regulatory elements. In addition, we found that six out of twenty-one BCP-ALL patients without t(11;14)(q24;q32) showed overexpression of miR-125b. Interestingly, four out of nine patients with *BCR/ABL*-positive BCP-ALL and one patient with B-cell lymphoid crisis that had progressed from chronic myelogenous leukemia overexpressed miR-125b. To examine the role of the deregulated expression of miR-125b in the development of B-cell tumor *in vivo*, we generated transgenic mice mimicking the t(11;14)(q24;q32) (Eμ/miR-125b-TG mice). Eμ/miR-125b-TG mice overexpressed miR-125b driven by *IGH* enhancer and promoter and developed IgM-negative or IgM-positive lethal B-cell malignancies with clonal proliferation. B cells obtained from the Eμ/miR-125b-TG mice were resistant to apoptosis induced by serum starvation. We identified *Trp53inp1*, a pro-apoptotic gene induced by cell stress, as a novel target gene of miR-125b in hematopoietic cells *in vitro* and *in vivo*. Our results provide direct evidence that miR-125b has important roles in the tumorigenesis of precursor B cells.**

Leukemia (2011) **25,** 1849–1856; doi:10.1038/leu.2011.166; published online 8 July 2011

Keywords: microRNA; mir-125; B-cell malignancies; transgenic mouse

Introduction

Chromosomal translocations involving the immunoglobulin heavy chain gene (*IGH*) locus have a pivotal role in the pathogenesis of human B-cell malignancies.[1,2] *IGH* translocation brings target genes positioned on different chromosome loci into close apposition with transcription elements within the *IGH* locus, resulting in deregulated expression of the target genes. The vast majority of the target genes physiologically act as key regulators in cell growth, differentiation, signal transduction or apoptosis of B cells.[1] Thus, deregulated expression of the translocated genes would alter B-cell fate leading to malignant transformation.

MicroRNAs (miRNAs) are small non-coding RNAs that regulate protein synthesis through degradation of messenger RNAs or inhibition of translation.[3,4] Many miRNAs are involved in a variety of important biological processes. Therefore, altered expression of miRNA affects cellular physiology and is responsible for some human disease.[5,6]

An evolutionally conserved miRNA, miR-125b, has been implicated in human cancers.[7–12] *MiR-125b-1*, mapped on *11q24*, has been found to be a target of recurrent chromosomal abnormalities seen in both lymphoid and myeloid malignancies.[7–10] We previously reported an insertion of *miR-125b-1* into the *IGH* locus in a patient with B-cell precursor acute lymphoblastic leukemia (BCP-ALL).[7] Subsequently, other groups identified fusion sequences of *IGH* and *miR-125b-1* from t(11;14)(q24;q32).[9,10] Bousquet *et al.*[8] identified *miR-125b-1* as a gene involved in t(2;11)(p21;q23) observed in patients with myelodysplastic syndrome and acute myeloid leukemia (AML). This translocation is associated with upregulation of miR-125b from 6- to 90-fold. Recent studies show that ectopic expression of miR-125b in hematopoietic stem cells developed several hematological malignancies.[13–15] However, *in vivo* oncogenic activities of miR-125b in B cells have not been fully understood.

In the present paper, we report molecular cloning of a novel breakpoint of t(11;14)(q24;q32) from a BCP-ALL patient, and show that transgenic mice mimicking this translocation develop lethal B-cell malignancies. Overexpression of miR-125b confers an anti-apoptotic property on cells along with inhibition of a pro-apoptotic gene, *Trp53inp1* (transformation-related protein 53 inducible nuclear protein 1), also known as *TP53INP1, TEAP, SIP* and *p53DINP1*,[16–19] at the mRNA and protein levels. Of clinical relevance, we found overexpression of miR-125b in a variety of hematological malignancies. In particular, its overexpression in *BCR/ABL*-positive BCP-ALL supports the result showing the cooperative function of miR-125b in BCR/ABL-induced leukemia in an animal model.[14]

Materials and methods

Molecular analyses of patients showing fusion between IGH and miR-125b-1

A novel t(11;14)(q24;q32) breakpoint was cloned by long distant-inverse PCR as described.[20] An IGH/miR-125b-1

Correspondence: Professor T Kitamura, Division of Cellular Therapy and Division of Stem Cell Signaling, The Institute of Medical Science, The University of Tokyo, 4-6-1 Shirokanedai, Minato-ku, Tokyo 108-8639, Japan. E-mail: kitamura@ims.u-tokyo.ac.jp
or Dr T Sonoki, Hematology/Oncology, Wakayama Medical University, 811-1 Kimi-idera, Wakayama 641-8510, Japan.
E-mail: sonoki@wakayama-med.ac.jp
Received 4 March 2011; revised 1 May 2011; accepted 17 May 2011; published online 8 July 2011

chimera transcript was yielded by reverse transcriptase–PCR (RT–PCR) using cDNA from leukemic cells of the insertion case. Primer pairs and conditions are described in 'Supplementary Materials and methods'.

Establishment of Eμ/miR-125b transgenic mice

A 422 bp of mouse genomic sequence including pre-miR-125b-1 was PCR amplified from C57BL/6 mouse genomic DNA. Primer pairs are described in 'Supplementary Materials and methods'. The fragment was inserted into the *Eco*RI site of pEμ/IGH plasmid (a kind gift from Dr Akagi, Saitama Cancer Institute, Japan). After digestion with *Xba*I and *Sal*I, the recombinant DNA was injected into 300 eggs at Unitech Laboratory (Chiba, Japan). Two F0 mice were successfully generated as stable TG mice and designated as TG116 and TG005.

Southern blot analysis of the IGHJ region of the Eμ/miR-125b-TG mice

Ten micrograms of genomic DNA was digested using *Eco*RI and subjected to Southern blot analysis using a digoxigenin-labeled 1.2 kb *Eco*RI/*Hin*dIII fragment of pMJH4 (JCRB, Osaka, Japan) recognizing the mouse IGHJ region.

Flow cytometric analysis

Red blood cell-depleted cells were stained with fluorescein isothiocyanate-conjugated anti-B220 Ab (Miltenyi Biotec, Gladbach, Germany), fluorescein isothiocyanate-conjugated anti-CD43 Ab (BD Biosciences, San Jose, CA, USA) or phycoerythrin-conjugated anti-CD19, IgM, CD3 and CD11b Abs (all from eBioscience, San Diego, CA, USA). For the apoptosis assay, cells were stained with fluorescein isothiocyanate AnnexinV and Propidium Iodide (BD Biosciences). Flow cytometric analysis was performed as described.[21,22]

Morphological analysis

Cytospin preparations of bone marrow (BM) cells or peripheral blood were stained with Giemsa. Images were obtained with a BX51 microscope and DP21 camera (Olympus, Tokyo, Japan). Formalin-fixed and paraffin-embedded sections were stained with hematoxylin–eosin and examined using a microscope (Axio Imager A1, Carl Zeiss, Jena, Germany) with an AxioCam camera and AxioVision 4.6 software (Carl Zeiss).

Purification of B220-positive cells

B220-positive cells of BM cells or splenocytes were selected using an anti-B220 bearing magnetic beads (CD45R (B220) MicroBeads; Miltenyi Biotec) and columns attached by magnetic fields (MACS Separation Columns; Miltenyi Biotec) according to the manufacturer's protocol.

Vector construction

MicroRNA expression fragments were cloned into pMXsEF1-(GFP), which were pMXs-based self-inactivating retrovirus vectors expressing miRNA under an EF1a promoter along with a BGH polyA site and expressing GFP under a PGK promoter along with a 3′ long terminal repeat. A miRNA expression cassette was constructed in the opposite direction from a GFP expression cassette. Expression fragments of miR-125b or IGH/miR-125b-1 were PCR amplified from C57BL/6 mouse genomic DNA or cDNA of tumor derived from a BCP-ALL patient,[7] respectively. Primer pairs are described in 'Supplementary Materials and methods'.

Real-time PCR

Total RNAs were treated with Deoxyribonuclease I (Invitrogen, Carlsbad, CA, USA) and reverse transcribed by using miScript Reverse Transcription Kit (QIAGEN, Hilden, Germany). Real-time PCR was performed using a LightCycler Workflow System (Roche Diagnostics, Mannheim, Germany). Mature miR-125b expression was measured using a miScript SYBR Green PCR kit (QIAGEN). cDNA was amplified with miR-125b-specific primers (QIAGEN). Expression of U6 small nuclear RNA, as an internal control, was used for normalization of the results. For mRNA real-time PCR, a SYBR Premix EX Taq (Takara, Shiga, Japan) was used as described.[23] Primer pairs are described in 'Supplementary Materials and methods'. Patients' informed consents were obtained in accordance with the Declaration of Helsinki, and the studies were approved by the ethics committees of Wakayama Medical University (approval no. 72-2009) and the University of Tokyo (approval no. 21-44-1224). Human blood, peripheral leukocytes total RNA (Clontech, Palo Alto, CA, USA) was used as a normal control. Total RNAs from peripheral blood of the patients were isolated using Mouse RiboPure-Blood RNA Isolation Kit (Ambion, Austin, TX, USA).

Luciferase assay

The 3′untranslated region (UTR) of the mouse Trp53inp1 was PCR amplified from C57BL/6 mouse genomic DNA. Primer pairs are described in 'Supplementary Materials and methods'. The 3′UTR was cloned to downstream of the *Renilla* luciferase stop codon in pGL4.74 vector (Promega, Madison, WI, USA). To generate the mutant 3′UTR of the mouse Trp53inp1, two-step PCR mutagenesis was performed[24–26] using the WT-3′UTR as a template. The Rluc-2 × 125b site vector contained two copies of a sequence designed to be perfectly complementary to the miR-125b downstream of the *Renilla* luciferase stop codon. 293T cells were co-transfected with the reporter vector (RLuc), miR-125b expression vector, and a transfection control vector expressing firefly luciferase (pGL3-control) using Fugene 6. Cells were harvested 30 h post-transfection and assayed with Dual Luciferase Assay (Promega). Three independent experiments were performed with a triplicate set.

Western blot analysis

Equal numbers of cells were lysed and western blotting was performed as described.[22,27,28] Anti-Trp53inp1 Ab (ANASPEC, Fremont, CA, USA) and anti-ERK1/2 Ab (Santa Cruz Biotechnology, Santa Cruz, CA, USA) were used.

Results

Overexpression of miR-125b in patients with BCP-ALL

We found a new BCP-ALL patient with t(11;14)(q24;q32) and cloned the breakpoint. In this patient, the translocation resulted in breakage in JH6 of *IGH* on chromosome *14q32* and fusion to its 12.6 kb downstream of the *miR-125b-1* locus on *11q24* (Figure 1a). The four breakpoints of the *11q24* so far identified by us and other groups[9,10] are clustered within 18 kb downstream of the *miR-125b-1* locus (Figure 1a). We previously reported a patient with BCP-ALL showing insertion of *miR-125b-1*

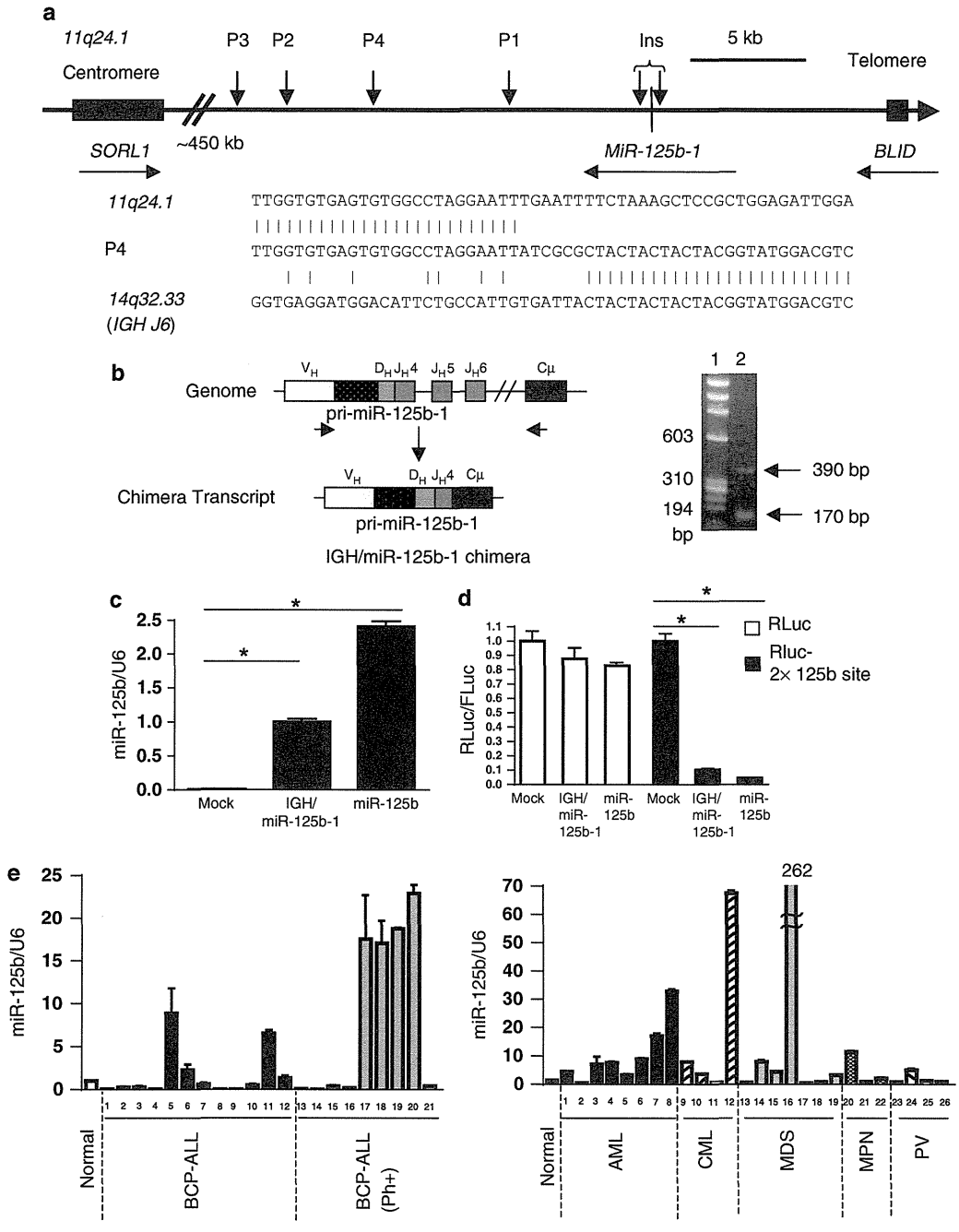

Figure 1 Molecular analyses of the expression of miR-125b in patients with BCP-ALL. (**a**) The *11q24* breakpoints cloned from BCP-ALL patients are clustered within 18 kb downstream of the *miR-125b-1* locus. Ins: Insertion points,[7] P1, P2 and P3 were previously reported.[9,10] P4 is a novel case showing t(11;14)(q24;q32). The nucleotide sequence cloned from P4 is shown. (**b**) The genome and chimera transcript structure observed in the insertion case.[7] RT–PCR using primers set at VH and Cμ produced two PCR products (390 and ~170 bp). (**c**) Relative expression levels of miR-125b were examined by real-time PCR in 293T cells transduced with pMXsEF1-IGH/miR-125b-1-(GFP), miR-125b expression vector (pMXsEF1-miR-125b-(GFP)) or mock (pMXsEF1-(GFP)). Data represent the average of two independent experiments. (**d**) *Renilla* luciferase (RLuc) vector or Rluc-2 × 125b site vector containing two copies of a sequence designed to be perfectly complementary to the miR-125b was co-transfected into 293T cells with a transfection control vector expressing firefly luciferase (pGL3 control) and pMXsEF1-IGH/miR-125b-1-(GFP), pMXsEF1-miR-125b-(GFP) or mock (pMXsEF1-(GFP)). Luciferase assays were performed with a triplicate set. (**e**) Relative expression levels of miR-125b were examined by real-time PCR in peripheral blood cells derived from patients with hematological diseases. Data represent the mean values ± s.e.m. of two independent experiments. *P*-values (*) of <0.05 were considered significant using a Student's two-tailed *t*-test. All data were representative of three independent experiments.

into a rearranged *IGH* allele.[7] The genomic structure of the *IGH* allele inserted by pri-miR-125b-1 sequence is shown in Figure 1b. RT–PCR using primer settings at VH and Cμ yielded 390 bp of chimera transcript consisting of VH, pri-miR-125b-1, DH, JH and Cμ, and ~170-bp product (Figure 1b; Supplementary Figure 1). Sequence analysis of the ~170-bp product revealed divers nucleotide alignments consisting of a VH/DH/JH/Cμ complex sequence, suggesting that this PCR product might originate from polyclonal B cells existing in the tumor sample. To examine whether this chimera transcript could produce mature miR-125b, we cloned the chimera sequence from the cDNA derived from the tumor cells into pMXsEF1-(GFP) (hereafter pMXsEF1-IGH/miR-125b-1-(GFP)). Real-time PCR confirmed that the cells transduced with pMXsEF1-IGH/miR-125b-1-(GFP), as well as a positive control, expressed miR-125b (Figure 1c). Furthermore, luciferase assay showed that miR-125b produced from IGH/miR-125b-1 repressed the activity of the reporter construct (Rluc-2 × 125b site) containing two copies of a sequence designed to be perfectly complementary to miR-125b (Figure 1d). These results demonstrated that the *IGH* allele inserted by the *miR-125b-1* sequence produces miR-125b when the promoter and enhancer are active.

For further analysis of the clinical relevance of miR-125b in hematological diseases, we examined expression of miR-125b in hematological tumors obtained from twenty-one BCP-ALL, eight AML, four chronic myelogenous leukemia, seven myelodysplastic syndrome, three myeloproliferative neoplasm and four polycythemia vera patients (Figure 1e; Supplementary Tables 1 and 2). We found that miR-125b was overexpressed in various patients; six BCP-ALL, five AML, two chronic myelogenous leukemia (accelerated phase and B-lymphoid blast crisis), one myeloproliferative neoplasm and two myelodysplastic syndrome patients showed more than fivefold higher expression of miR-125b compared with normal samples. Of note, miR-125b was highly expressed in four out of nine t(9;22)(q34;q11) positive BCP-ALL and one B-lymphoid blast crisis derived from chronic myelogenous leukemia.

We also investigated expression of miR-125a possessing the same seed sequence as that of miR-125b in these patients (Supplementary Figure 2). We found that one BCP-ALL patient showed more than fivefold higher expression of miR-125a compared with normal samples. These results indicate that overexpression of miR-125a in hematological malignancies is infrequent.

Eμ/miR-125b-TG mice developed lethal lymphoid malignancies

We next generated Eμ/miR-125b-TG mice to investigate whether deregulated expression of miR-125b could be responsible for the development of B-cell malignancy *in vivo*. The transgene consisted of human intronic enhancer of *IGH* (Eμ), mouse VH promoter and rabbit β-globin-including mouse genomic sequence containing pre-miR-125b (Supplementary Figure 3a). Since the VH promoter and the Eμ enhancer become active at the late pro-B cell stage,[29] miR-125b is thought to be expressed at this differentiation stage. We examined two TG lines, designated as Eμ/miR-125b-TG116 (TG116) and Eμ/miR-125b-TG005 (TG005). Southern blot analysis using a transgene-specific probe showed different patterns of integration, suggesting that a high copy number was introduced in TG116 compared with TG005 (Supplementary Figure 3). We confirmed expression of miR-125b in both TG mice (Figure 2a). All TG116 mice developed lethal lymphoid tumors within 35 weeks whereas five out of thirteen TG005 mice died within 50 weeks with a disease similar to that of TG116 (Figure 2b). When the disease became overt, both TG116 and TG005 mice showed splenomegaly (Figure 2c; Supplementary Figure 4). Moreover, TG116 mice showed hepatomegaly and an increased number of BM cells, whereas the concentration of hemoglobin (Hb) of both TG116 and TG005 mice decreased compared with that of wild-type (WT) mice with statistical significance (Supplementary Figure 4).

Tumor cells with morphologically lymphoblastic features appeared in BM and peripheral blood (Figure 2d). Histological examination showed that atypical lymphoid cells filled the spleen and infiltrated the liver (Figure 2d). Using flow cytometric analysis, we found that nine morbid TG116 mice had developed IgM^- precursor B-cell tumors, one IgM^+ B-cell tumor and one T-cell tumor, whereas four morbid TG005 mice had developed IgM^+ B-cell tumors and one $IgM^+/B220^-$ tumor (Figure 2e and data not shown). Flow cytometric analysis delineated that most tumor cells of the morbid TG116 mice consisted of $B220^+/CD19^+/IgM^-/CD43^+$ B cells, whereas those of the morbid TG005 mice were $B220^+/CD19^+/IgM^+/CD43^-$ B cells. The number of $B220^+/CD19^+/IgM^-/CD43^+$ B cells increased in the TG116 mice as early as 4 weeks mice (Supplementary Figure 5a). To examine the tumor clonality, we performed Southern blot analysis; we detected rearranged bands in eight out of nine morbid TG116 mice and in all the five morbid TG005 mice, indicating clonal proliferation of B cells (Figure 2f and data not shown). One out of four young TG116 mice showed clonal rearranged bands before the onset of the disease, suggesting that clonal proliferation can occur even in 4 weeks after birth (Supplementary Figure 5b). Collectively, Eμ/miR-125b-TG mice developed lethal IgM^- or IgM^+ B-cell malignancies with clonal expansion.

MiR-125b inhibited apoptosis of hematopoietic cells

We next analyzed the mechanism by which miR-125b promoted leukemogenesis *in vivo*. To identify target genes of miR-125b, we performed a bioinformatics search using Targetscan (http://www.targetscan.org/). There were some apoptosis-related genes, such as *Bak1*, *Bmf*, *KLF13*, *MCL-1* and *Trp53inp1*, among the candidate target genes of miR-125b. In addition, we performed microarray analysis of 32Dcl3 cells transduced with miR-125b or mock. In microarray analysis, we found that among the candidate target genes the expression levels of Trp53inp1 mRNAs were reduced in 32Dcl3 cells transduced with miR-125b (data not shown). The 3′UTR of Trp53inp1 contained one putative target site that matched the seed sequences of miR-125b. *Trp53inp1* is a pro-apoptotic gene induced by cell stress,[16–19] and its repression is involved in tumorigenesis.[30,31] To confirm that *Trp53inp1* is a direct target gene of miR-125b, the wild-type 3′UTR of Trp53inp1 or the mutated 3′UTR was cloned to downstream of the *Renilla* luciferase open reading frame (Figure 3a). We performed luciferase assays and found that miR-125b directly represses the expression of the reporter gene with the Trp53inp1-3′UTR but not that with mutated 3′UTR of Trp53inp1 (Figure 3a).

We then examined the expression levels of Trp53inp1 mRNAs in 32Dcl3 cells at different time intervals after inducing apoptosis by IL-3 withdrawal (Supplementary Figure 6a). We found that the expression levels of Trp53inp1 mRNAs increased after inducing apoptosis by IL-3 withdrawal but that those of Trp53inp1 mRNAs were repressed in miR-125b-transduced 32Dcl3 cells compared with mock-transduced 32Dcl3 cells at each time point. In addition, the numbers of apoptotic cells decreased in miR-125b-transduced cells but not in miR-30a,

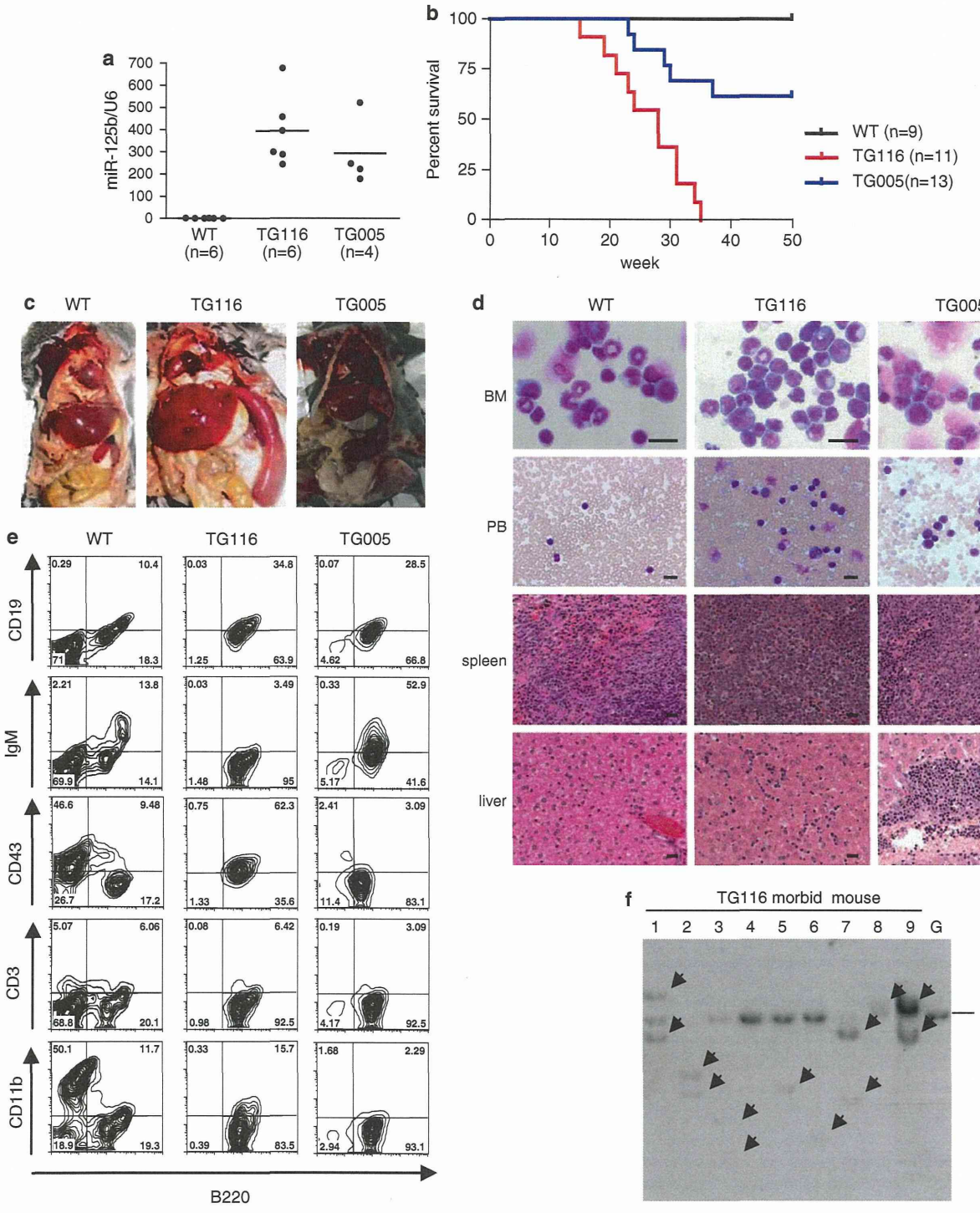

Figure 2 Eμ/miR-125b-TG mice developed lethal B-cell tumors. (**a**) Relative expression levels of miR-125b were examined by real-time PCR in B220-positive BM cells derived from Eμ/miR-125b-TG (TG116 and TG005) or WT mice. Data represent the average of two independent experiments. (**b**) Kaplan–Meier analysis for the survival of TG116, TG005 and WT mice. (**c**) Both TG116 and TG005 mice exhibit splenomegaly. (**d**) Cytospin preparations of BM cells and peripheral blood smears obtained from TG116, TG005 or WT mice were stained with Giemsa. Hematoxylin and eosin staining of spleen and liver obtained from TG116, TG005 or WT mice. Bars, 20 μm. (**e**) Flow cytometric analysis of BM cells derived from morbid TG116, morbid TG005 or WT mice. (**f**) Southern blot analysis of splenocytes derived from morbid TG116 mice (lanes 1–9). Clonal rearranged bands (arrows) were detected in lanes 1–3 and 5–9. G, germ line control.

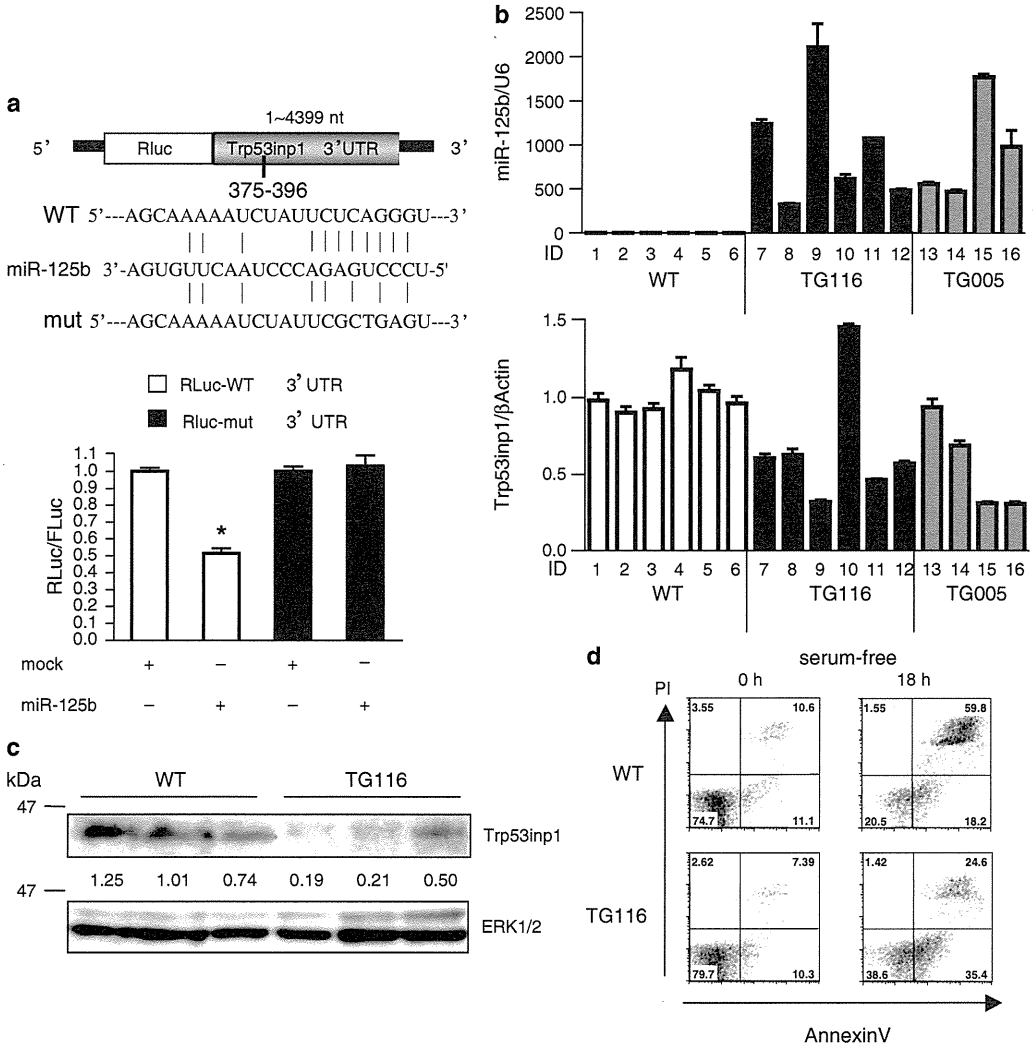

Figure 3 MiR-125b repressed expression of Trp53inp1 and inhibited apoptosis of B cells. (**a**) 293T cells were co-transfected with a transfection control vector (pGL3-control) and pMXsEF1-miR-125b-(GFP) or mock (pMXsEF1-(GFP)). Luciferase assays were performed with a triplicate set. (**b**) Relative expression levels of miR-125b were examined by real-time PCR in purified B220-positive splenocytes derived from TG116 mice (mouse IDs 7–12), TG005 mice (mouse IDs 13–16) or WT mice (mouse IDs 1–6) (upper panel). Data points correspond to the mean values ± s.e.m. of two independent experiments. Relative expression levels of Trp53inp1 in these cells were examined by real-time PCR. Data points correspond to the mean values ± s.e.m. of three independent experiments. (**c**) Expression of Trp53inp1 protein in purified B220-positive splenocytes of TG116 mice (lanes 4–6) or WT mice (lanes 1–3). Lysates were immunoblotted with anti-Trp53inp1 Ab or anti-ERK1/2 Ab as a control. Relative band intensities of Trp53inp1 were calculated by densitometric analysis and normalized to ERK1/2. (**d**) Purified B220-positive splenocytes of 20-week-old TG116 or WT mice were cultured without serum. Cells were stained with fluorescein isothiocyanate AnnexinV and Propidium Iodide. *P*-values (*) of <0.05 were considered significant using a Student's two-tailed *t*-test. All data were representative of three independent experiments.

used as a control miRNA, or mock-transduced cells (Supplementary Figure 6b). Moreover, expression levels of mature miR-125b and Trp53inp1 mRNA were inversely correlated. With one exception (Figure 3b, lane 10), TG116 mice tended to express lower levels of Trp53inp1 at the mRNA and protein levels compared with WT mice (Figures 3b and c). We also found that B220-positive splenocytes derived from TG116 mice became resistant to apoptosis induced by serum starvation when compared with WT mice (Figure 3d). Collectively, these results indicated that miR-125b inhibits apoptosis of hematopoietic cells at least partly through repressing Trp53inp1.

Discussion

A number of miRNAs are located on regions of the genome involved in chromosome alteration, such as deletion, amplification and translocation as observed in various malignant tumors.[5,6] Although cloned chromosomal translocations involving *IGH* loci are common genomic alterations in B-cell malignancies, only *miR-125b-1* has so far been shown to be a target miRNA related to *IGH* translocations. In the present paper, we report a new patient with t(11;14)(q24;q32) and direct evidence for the oncogenic potential of miR-125b in B cells using transgenic mice mimicking the translocation.

Overexpression of miR-125b in BM cells was reported to induce myeloproliferative neoplasm in transplanted mice that progressed to AML,[13] while BM-derived highly purified hematopoietic stem cells overexpressing miR-125b tended to differentiate into lymphoid lineages after transplantation.[15] On the other hand, half of the mice transplanted with miR-125b-overexpressing fetal liver hematopoietic stem cells developed T-ALL, B-ALL or myeloproliferative neoplasm.[14] These report indicated that miR-125b has important roles in proliferation and differentiation of hematopoietic stem cells. However, the functions of miR-125b in B cells have remained elusive.

In the present paper, we have shown that overexpression of miR-125b triggered by *IGH* enhancer and promoter induces two different types of lethal B-cell malignancies. TG116 mice mainly develop faster-onset IgM-negative tumors and TG005 mice develop slower-onset IgM-positive tumors. This difference could be explained by expression levels of miR-125b due to the different copy number of transgenes integrated into mouse chromosome (Supplementary Figure 3b). Alternatively, other factors such as epigenetic changes or inhibition of other miRNAs might have been involved in the development of the disease and were responsible for the difference in the disease phenotypes.

MiR-125 was suggested to confer anti-apoptotic characteristics on cells by reducing expression levels of apoptosis-inducing genes such as *Bak1*, *Bmf* and *KLF13* in mouse hematopoietic cells.[15,32] In this study, we have identified *Trp53inp1* as a novel candidate of the miR-125b target gene in mice; its mRNA and protein levels decreased in B220-positive cells obtained from Eμ/miR-125b-TG mice. Indeed, Trp53inp1 null mice were shown to be susceptible to cancer development.[31]

Of clinical relevance, we found that miR-125b was overexpressed in various hematopoietic diseases including BCP-ALL, AML and myelodysplastic syndrome without chromosomal translocations, t(11;14)(q24;q32) or t(2;11)(p21;q23). Mature miR-125b is also produced from *miR-125b-2* mapped on *21q21*. However, the above-mentioned patients except for a BCP-ALL patient ID 7 showed no abnormalities of chromosome 21 (Supplementary Tables 1 and 2). These cases may express high amount of miR-125b by unknown mechanisms. Interestingly, we reported here that four out of nine *BCR/ABL*-positive ALL patients and one with B-cell lymphoid crisis of chronic myelogenous leukemia showed high expression levels of miR-125b. Another group also independently found overexpression of miR-125b in a *BCR/ABL*-positive ALL patient lacking t(11;14)(q24;q32).[9] Recently, it was reported that miR-125b can cooperate in leukemogenic activity with BCR/ABL. Taking clinical and experimental results together, overexpression of miR-125b would be associated with hematological malignancies. As inactivation of oncomiR, such as miR-21, can decrease tumorigenesis,[33] inhibition of miR-125b could be a new strategy for treatment of hematopoietic malignancies. Our transgenic mice will be a useful tool in the development of the therapy for the patients with high miR-125b expression.

Conflict of interest

The authors declare no conflict of interest.

Acknowledgements

We thank Dr Kiwamu Akagi (Saitama Cancer Institute, Japan) for providing the pEμ/IGH plasmid, Dr Hiroshi Matsuoka (Kobe University, Japan) for helpful discussion and Dr Dovie Wylie for her excellent language support. This work was supported by grants from the Ministry of Education, Culture, Sports, Science and Technology (MEXT), Japan, and was in part supported by Grant-in-Aid for Scientific Research on Innovative Areas, Global COE Program 'Center of Education and Research for the Advanced Genome-Based Medicine—For personalized medicine and the control of worldwide infectious diseases', MEXT, Japan, Grant for Basic and Clinical Research Project from Osaka Cancer Research Foundation 2008, A Research Grant on Priority Areas from Wakayama Medical University 2008, and a grant from the Japan Society for the Promotion Science (JSPS). This work was performed in the Cooperative Research Project of the Institute of Medical Science, Tokyo University. YE is a JSPS research fellow.

References

1 Willis TG, Dyer MJ. The role of immunoglobulin translocations in the pathogenesis of B-cell malignancies. *Blood* 2000; **96**: 808–822.
2 Küppers R, Dalla-Favera R. Mechanisms of chromosomal translocations in B cell lymphomas. *Oncogene* 2001; **20**: 5580–5594.
3 Ambros V. The functions of animal microRNAs. *Nature* 2004; **431**: 350–355.
4 Bartel D. MicroRNAs: genomics, biogenesis, mechanism, and function. *Cell* 2004; **116**: 281–297.
5 Medina PP, Slack FJ. microRNAs and cancer: an overview. *Cell Cycle* 2008; **7**: 2485–2492.
6 Iorio MV, Croce CM. MicroRNAs in cancer: small molecules with a huge impact. *J Clin Oncol* 2009; **27**: 5848–5856.
7 Sonoki T, Iwanaga E, Mitsuya H, Asou N. Insertion of microRNA-125b-1, a human homologue of lin-4, into a rearranged immunoglobulin heavy chain gene locus in a patient with precursor B-cell acute lymphoblastic leukemia. *Leukemia* 2005; **19**: 2009–2010.
8 Bousquet M, Quelen C, Rosati R, Mansat-De Mas V, La Starza R, Bastard C *et al*. Myeloid cell differentiation arrest by miR-125b-1 in myelodysplastic syndrome and acute myeloid leukemia with the t(2;11)(p21;q23) translocation. *J Exp Med* 2008; **205**: 2499–2506.
9 Chapiro E, Russell L, Struski S, Cavé H, Radford-Weiss I, Valle V *et al*. A new recurrent translocation t(11;14)(q24;q32) involving IGH@ and miR-125b-1 in B-cell progenitor acute lymphoblastic leukemia. *Leukemia* 2010; **24**: 1362–1364.
10 Tassano E, Acquila M, Tavella E, Micalizzi C, Panarello C, Morerio C. MicroRNA-125b-1 and BLID upregulation resulting from a novel IGH translocation in childhood B-Cell precursor acute lymphoblastic leukemia. *Genes Chromosomes Cancer* 2010; **49**: 682–687.
11 Gefen N, Binder V, Zaliova M, Linka Y, Morrow M, Novosel A *et al*. Hsa-mir-125b-2 is highly expressed in childhood ETV6/RUNX1 (TEL/AML1) leukemias and confers survival advantage to growth inhibitory signals independent of p53. *Leukemia* 2010; **24**: 89–96.
12 Klusmann J, Li Z, Böhmer K, Maroz A, Koch M, Emmrich S *et al*. miR-125b-2 is a potential oncomiR on human chromosome 21 in megakaryoblastic leukemia. *Genes Dev* 2010; **24**: 478–490.
13 O'Connell R, Chaudhuri A, Rao D, Gibson W, Balazs A, Baltimore D. MicroRNAs enriched in hematopoietic stem cells differentially regulate long-term hematopoietic output. *Proc Natl Acad Sci USA* 2010; **107**: 14235–14240.
14 Bousquet M, Harris MH, Zhou B, Lodish HF. MicroRNA miR-125b causes leukemia. *Proc Natl Acad Sci USA* 2010; **107**: 21558–21563.
15 Ooi AG, Sahoo D, Adorno M, Wang Y, Weissman IL, Park CY. MicroRNA-125b expands hematopoietic stem cells and enriches for the lymphoid-balanced and lymphoid-biased subsets. *Proc Natl Acad Sci USA* 2010; **107**: 21505–21510.
16 Tomasini R, Samir A, Carrier A, Isnardon D, Cecchinelli B, Soddu S *et al*. TP53INP1s and homeodomain-interacting protein kinase-2 (HIPK2) are partners in regulating p53 activity. *J Biol Chem* 2003; **278**: 37722–37729.

17 Tomasini R, Samir A, Vaccaro M, Pebusque M, Dagorn J, Iovanna J *et al.* Molecular and functional characterization of the stress-induced protein (SIP) gene and its two transcripts generated by alternative splicing. SIP induced by stress and promotes cell death. *J Biol Chem* 2001; **276**: 44185–44192.
18 Tomasini R, Samir A, Pebusque M, Calvo E, Totaro S, Dagorn J *et al.* P53-dependent expression of the stress-induced protein (SIP). *Eur J Cell Biol* 2002; **81**: 294–301.
19 Okamura S, Arakawa H, Tanaka T, Nakanishi H, Ng CC, Taya Y *et al.* p53DINP1, a p53-inducible gene, regulates p53-dependent apoptosis. *Mol Cell* 2001; **8**: 85–94.
20 Akasaka T, Balasas T, Russell LJ, Sugimoto KJ, Majid A, Walewska R *et al.* Five members of the CEBP transcription factor family are targeted by recurrent IGH translocations in B-cell precursor acute lymphoblastic leukemia (BCP-ALL). *Blood* 2007; **109**: 3451–3461.
21 Kato N, Kitaura J, Doki N, Komeno Y, Watanabe-Okochi N, Togami K *et al.* Two types of C/EBPα mutations play distinct but collaborative roles in leukemogenesis: lessons from clinical data and BMT models. *Blood* 2011; **117**: 221–233.
22 Watanabe-Okochi N, Oki T, Komeno Y, Kato N, Yuji K, Ono R *et al.* Possible involvement of RasGRP4 in leukemogenesis. *Int J Hematol* 2009; **89**: 470–481.
23 Enomoto Y, Yamanishi Y, Izawa K, Kaitani A, Takahashi M, Maehara A *et al.* Characterization of leukocyte mono-immunoglobulin-like receptor 7 (LMIR7)/CLM-3 as an activating receptor: its similarities to and differences from LMIR4/CLM-5. *J Biol Chem* 2010; **285**: 35274–35283.
24 Izawa K, Kitaura J, Yamanishi Y, Matsuoka T, Oki T, Shibata F *et al.* Functional analysis of activating receptor LMIR4 as a counterpart of inhibitory receptor LMIR3. *J Biol Chem* 2007; **282**: 17997–18008.
25 Izawa K, Kitaura J, Yamanishi Y, Matsuoka T, Kaitani A, Sugiuchi M *et al.* An activating and inhibitory signal from an inhibitory receptor LMIR3/CLM-1: LMIR3 augments lipopolysaccharide response through association with FcRgamma in mast cells. *J Immunol* 2009; **183**: 925–936.
26 Yamanishi Y, Kitaura J, Izawa K, Matsuoka T, Oki T, Lu Y *et al.* Analysis of mouse LMIR5/CLM-7 as an activating receptor: differential regulation of LMIR5/CLM-7 in mouse versus human cells. *Blood* 2008; **111**: 688–698.
27 Ono R, Nakajima H, Ozaki K, Kumagai H, Kawashima T, Taki T *et al.* Dimerization of MLL fusion proteins and FLT3 activation synergize to induce multiple-lineage leukemogenesis. *J Clin Invest* 2005; **115**: 919–929.
28 Komeno Y, Kitaura J, Watanabe-Okochi N, Kato N, Oki T, Nakahara F *et al.* AID-induced T-lymphoma or B-leukemia/lymphoma in a mouse BMT model. *Leukemia* 2010; **24**: 1018–1024.
29 Costinean S, Zanesi N, Pekarsky Y, Tili E, Volinia S, Heerema N *et al.* Pre-B cell proliferation and lymphoblastic leukemia/high-grade lymphoma in E(mu)-miR155 transgenic mice. *Proc Natl Acad Sci USA* 2006; **103**: 7024–7029.
30 Gironella M, Seux M, Xie M, Cano C, Tomasini R, Gommeaux J *et al.* Tumor protein 53-induced nuclear protein 1 expression is repressed by miR-155, and its restoration inhibits pancreatic tumor development. *Proc Natl Acad Sci USA* 2007; **104**: 16170–16175.
31 Gommeaux J, Cano C, Garcia S, Gironella M, Pietri S, Culcasi M *et al.* Colitis and colitis-associated cancer are exacerbated in mice deficient for tumor protein 53-induced nuclear protein 1. *Mol Cell Biol* 2007; **27**: 2215–2228.
32 Guo S, Lu J, Schlanger R, Zhang H, Wang JY, Fox MC *et al.* MicroRNA miR-125a controls hematopoietic stem cell number. *Proc Natl Acad Sci USA* 2010; **107**: 14229–14234.
33 Medina PP, Nolde M, Slack FJ. OncomiR addiction in an *in vivo* model of microRNA-21-induced pre-B-cell lymphoma. *Nature* 2010; **467**: 86–90.

Supplementary Information accompanies the paper on the Leukemia website (http://www.nature.com/leu)

blood

2011 117: 221-233
Prepublished online September 30, 2010;
doi:10.1182/blood-2010-02-270181

Two types of C/EBPα mutations play distinct but collaborative roles in leukemogenesis: lessons from clinical data and BMT models

Naoko Kato, Jiro Kitaura, Noriko Doki, Yukiko Komeno, Naoko Watanabe-Okochi, Katsuhiro Togami, Fumio Nakahara, Toshihiko Oki, Yutaka Enomoto, Yumi Fukuchi, Hideaki Nakajima, Yuka Harada, Hironori Harada and Toshio Kitamura

Blood (print ISSN 0006-4971, online ISSN 1528-0020), is published weekly by the American Society of Hematology, 2021 L St, NW, Suite 900, Washington DC 20036.

Two types of C/EBPα mutations play distinct but collaborative roles in leukemogenesis: lessons from clinical data and BMT models

Naoko Kato,[1,2] Jiro Kitaura,[1] Noriko Doki,[1] Yukiko Komeno,[1] Naoko Watanabe-Okochi,[3] Katsuhiro Togami,[1] Fumio Nakahara,[1,2] Toshihiko Oki,[1,2] Yutaka Enomoto,[1] Yumi Fukuchi,[4] Hideaki Nakajima,[4] Yuka Harada,[5] Hironori Harada,[6] and Toshio Kitamura[1,2]

Divisions of [1]Cellular Therapy and [2]Stem Cell Signaling, Institute of Medical Science, University of Tokyo, Tokyo, Japan; [3]Department of Hematology and Oncology, Graduate School of Medicine, University of Tokyo, Tokyo, Japan; [4]Division of Hematology, Department of Internal Medicine, Keio University School of Medicine, Tokyo, Japan; [5]International Radiation Information Center, Research Institute for Radiation Biology and Medicine, Hiroshima University, Hiroshima, Japan; and [6]Department of Hematology and Oncology, Research Institute for Radiation Biology and Medicine, Hiroshima University, Hiroshima, Japan

Two types of mutations of a transcription factor CCAAT-enhancer binding protein α (C/EBPα) are found in leukemic cells of 5%-14% of acute myeloid leukemia (AML) patients: N-terminal mutations expressing dominant negative p30 and C-terminal mutations in the basic leucine zipper domain. Our results showed that a mutation of C/EBPα in one allele was observed in AML after myelodysplastic syndrome, while the 2 alleles are mutated in de novo AML. Unlike an N-terminal frame-shift mutant (C/EBPα-N^m)–transduced cells, a C-terminal mutant (C/EBPα-C^m)–transduced cells alone induced AML with leukopenia in mice 4-12 months after bone marrow transplantation. Coexpression of both mutants induced AML with marked leukocytosis with shorter latencies. Interestingly, C/EBPα-C^m collaborated with an Flt3-activating mutant Flt3-ITD in inducing AML. Moreover, C/EBPα-C^m strongly blocked myeloid differentiation of 32Dcl3 cells, suggesting its class II mutation-like role in leukemogenesis. Although C/EBPα-C^m failed to inhibit transcriptional activity of wild-type C/EBPα, it suppressed the synergistic effect between C/EBPα and PU.1. On the other hand, C/EBPα-N^m inhibited C/EBPα activation in the absence of PU.1, despite low expression levels of p30 protein generated by C/EBPα-N^m. Thus, 2 types of C/EBPα mutations are implicated in leukemogenesis, involving different and cooperating molecular mechanisms. (*Blood.* 2011; 117(1):221-233)

Introduction

The CCATT/enhancer binding protein α (C/EBPα) transcription factor is a critical regulator of proliferation and differentiation in myeloid cells.[1,2] C/EBPα consists of an N-terminal transcriptional activation domain and a C-terminal basic leucine zipper (bZIP) domain.[3-5] Two isoforms of C/EBPα proteins are generated from different translation start sites: a full-length 42-kDa protein (p42) and a truncated 30-kDa protein (p30) that lacks an N-terminal transcriptional activation domain. C/EBPα-p30 isoform inhibits C/EBPα-p42–mediated transcription.[6-8] Importantly, C/EBPα promotes differentiation both by up-regulation of lineage-specific gene products[9-11] and by proliferation arrest.[12] Recent studies have indicated that C/EBPα-induced growth arrest is regulated by its interaction with other molecules involved in growth control: E2F,[13-15] Max,[16] and SWI/SNF chromatin remodeling complexes.[17] For example, repression of E2F activity by E2F-C/EBPα interaction results in the down-regulation of c-Myc, leading to granulocytic differentiation.[18,19]

According to several studies, *CEBPA* mutations are found in 5%-14% of acute myeloid leukemia (AML) patients belonging to the French-American-British subtypes M1, M2, or in some cases M4.[8,20-22] The mutations of the *CEBPA* gene can be largely categorized into 2 types: one is an N-terminal frame-shift mutation disrupting p42 and producing p30 as a major product, and the other is a C-terminal in-frame mutation disrupting the bZIP region. Interestingly, most AML patients with *CEBPA* mutations have both mutations simultaneously,[23-25] and such patients displayed a favorable outcome.[22,26] On the other hand, AML patients with single *CEBPA* mutations did not express a distinctive signature, presumably due to a variety of associating gene alterations, including Flt3 activating mutations. Related to this, involvement of single *CEBPA* mutations with myelodysplastic syndrome (MDS) remains to be clarified.[27,28]

Analysis of mice with genetic alterations in the *CEBPA* locus has contributed to delineation of molecular mechanisms by which *CEBPA* mutations induce leukemia. Conditional deficiency of C/EBPα led to a differentiation block at the transition between common myeloid progenitors and granulocyte/monocyte progenitors but not to development of leukemia.[1] However, Cebpa$^{L/L}$ mice, expressing only p30 as C/EBPα protein, developed myeloid leukemia with complete penetration.[29] On the other hand, Cebpa$^{BRM2/BRM2}$ mice, carrying a point mutation in the bZIP domain that dampened E2F interaction, showed only preleukemic features.[14] Interestingly, the same group has recently reported combinational effects of the C-terminal and the N-terminal mutations on leukemogenesis by using Cebpa$^{L/L}$ mice, Cebpa$^{K/K}$ mice carrying the K313 duplication in the C-terminal domain, and Cebpa$^{K/L}$ mice.[29,30] They proposed that efficient leukemogenesis is caused by the combination of both premalignant HSC expansion induced by

Submitted February 17, 2010; accepted September 22, 2010. Prepublished online as *Blood* First Edition paper, September 30, 2010; DOI 10.1182/blood-2010-02-270181.

The online version of this article contains a data supplement.

The publication costs of this article were defrayed in part by page charge payment. Therefore, and solely to indicate this fact, this article is hereby marked "advertisement" in accordance with 18 USC section 1734.

C-terminal *CEBPA* mutation and residual myeloid lineage commitment maintained by the N-terminal *CEBPA* mutation.[30]

Causative gene alterations in hematologic malignancies have been extensively studied, and it is now recognized that multiple mutations contribute to development of leukemia. These gene alterations are categorized into 2 groups, class I and class II mutations.[31,32] Class I mutations include activating mutations of *FLT3*, *C-KIT*, *JAK2*, *SHP2*, and *RAS*, or inactivating mutations of *TP53* and *NF-1*, and induce proliferation or block apoptosis of hemopoietic cells. On the other hand, class II mutations disrupt normal functions of transcription factors and chromosome-modifying enzymes including *MLL*, *RUNX1*, *RARA*, and *PU.1* and hamper differentiation of hemopoietic cells. Combinations of class I and class II mutations are frequently observed in patients' leukemic cells.[33,34] In addition, we and others presented evidence that class I and class II mutations collaborate in the development of leukemia in mouse models.[35,36] Among a variety of gene alterations found in leukemia, *CEBPA* mutations are unique because different *CEBPA* mutations are frequently found on different alleles in leukemic cells of de novo AML.[22-26]

In the present study, we searched for mutations of the *CEBPA* gene in patients with myeloid malignancies, and found N- and C-terminal double mutations in patients with de novo AML. In patients with MDS/AML or therapy-related AML or MDS, only N- or C-terminal single mutation was identified. We chose a C-terminal mutation 304_323dup (hereafter called C/EBPα-C^m) and an N-terminal mutation (T60fsX159) (hereafter C/EBPα-N^m) for further analysis that had been isolated as double *CEBPA* mutations in a de novo AML patient. To evaluate the effects of these mutations on leukemogenesis, we used a mouse bone marrow transplantation (BMT) model. Interestingly, unlike the phenotype in $Cebpa^{K/K}$, $Cebpa^{K/+}$, $Cebpa^{BRM2/BRM2}$, or $Cebpa^{BRM2/+}$ mice,[14,29,30] C/EBPα-C^m alone induced AML with leukopenia in transplanted mice after BMT. We also confirmed the efficient induction of AML by coexpression of C/EBPα-C^m and C/EBPα-N^m. We will discuss the possible molecular mechanisms by which C/EBPα-N^m worked in concert with C/EBPα-C^m in accelerating leukemogenesis.

Methods

Patients and samples

We chose patients with hematologic diseases (224 MDS/AML patients, 71 therapy-related AML or MDS patients, and 89 de novo AML patients, who had been diagnosed at Hiroshima University Hospital between 1985 and 2007, are not a consecutive series of patients). All studies were approved by the Institutional Review Board at Hiroshima University and the ethics committee of the University of Tokyo (approval no. 20-10-0620). Patients' informed consents were obtained in accordance with the Declaration of Helsinki. *CEBPA* mutation screening by polymerase chain reaction (PCR)–single strand conformation polymorphism analysis and identification of *CEBPA*, *AML1*, *N-RAS*, *FLT3*, *PTPN11*, *C-KIT*, and *TP53* mutations was performed as described previously.[37]

Retroviral vectors

We used 2 C/EBPα mutants, N^m or C^m, as well as C/EBPα wild-type (WT) and C/EBPα N-terminal truncated p30 (p30). C/EBPα-WT, p30, N^m, or C^m, which was tagged with a FLAG or Myc epitope at the C terminus, was inserted upstream of the internal ribosome entry site-enhanced green fluorescent protein (IRES-EGFP) cassette of pMYs-IG to generate pMYs-FLAG or Myc-tagged CEBPα-WT, p30, N^m, or C^m-IG, respectively. Similarly, these fragments were subcloned into pMXs-IRES-puro (pMXs-IP), pMXs-IRES-blasticidin (pMXs-IB), or pMYs-IRES-dsRED (pMYs-IR). Flt3-ITD cDNA, which was derived from patient's leukemic cells harboring a 20-amino acid tandem duplication called M3[38,39] was subcloned into pMYs-IG to generate pMYs-Flt3-ITD-IG. Human granulocyte colony-stimulating factor receptor (G-CSF-R) cDNA, a kind gift from Dr Shigekazu Nagata (Kyoto University, Kyoto, Japan), was subconed into pMXs-IB to generate pMXs-G-CSF-R-IB.

Retroviral infection was done as described previously.[40] Briefly, retroviruses were generated by transient transfection of Plat-E packaging cells with FuGENE 6 (Roche Diagnostics).[41,42] Growth of transduced 32Dcl3 cells, which were subject to the drug selection with 1 μg/mL puromycin or 10 μg/mL blasticidin, was estimated by quantitating luminescence as described previously.[43]

Flow cytometric analysis

Briefly, cells were stained with phycoerythrin-conjugated antibodies (Abs) or biotinylated Abs and phycoerythrin/Cy5-streptavidin (eBioscience). Flow cytometric analysis of the stained cells was performed with FACSCalibur flow (BD Biosciences) equipped with FlowJo Version 7.2.4 software (TreeStar).

Real-time reverse-transcription PCR

Real-time reverse-transcription (RT) PCR was performed as described previously.[40] Reaction was subject to one cycle of 95°C for 30 seconds, 45 cycles of PCR at 95°C for 5 seconds, 55°C for 10 seconds, and 72°C for 10 seconds. The following primer pairs were used: 5′-AAGGCCCAGTGTGTCTCTGT-3′ (forward), and 5′-TACCAGCCCCAACTCAAAAC-3′ (reverse) for G-CSF-R, 5′-AGAGGGAAATCGTGCGTGAC-3′ (forward), and 5′-CAATAGTGATGACCTGGCCGT-3′ (reverse) for β-actin, 5′-GCCCCTAGTGCTGCATGAG-3′ (forward) and 5′-CCACAGACACCACATCAATTTCTT-3′ (reverse) for c-Myc.

Western blot analysis

Equal numbers of cells were lysed and Western blotting was performed as described previously.[35,40] Anti-Flag (M2) Ab (Sigma-Aldrich), anti-c-Myc (9E10) Ab (Roche Diagnostics), anti-C/EBPα (14AA) or (N-19) Ab (Santa Cruz Biotechnology), ERK1/2, signal transducer and activator of transcription (STAT)3, STAT5, AKT1, or Flt3 Abs, and phospho-STAT3 Ab (Santa Cruz Biotechnology), anti-phospho mitogen-activated protein kinase and phospho-AKT Abs (Cell Signaling Technology), and phospho-STAT5 Ab (BD Biosciences) were used.

Luciferase assay

The 293T cells were transiently transfected with the luciferase reporter plasmid p(C/EBP)2TK (kindly provided by Atsushi Iwama, Chiba University, Japan), pMXs-C/EBPα-WT or mutants-IP, and pEF-BOS/PU.1 for C/EBPα transcriptional activity, or E2Fx6-TATA-LUC, pCMV-E2F1, and pCMV-DP1 (kindly provided by Claus Nerlov, EMBL Mouse Biology Unit, Italy) for E2F transcriptional activity.[15] Luciferase assays were performed by Dual luciferase assay systems (Promega).

Immunostaining

Immunostaining of 293T cells transiently transfected with retrovirus constructs was performed as described previously.[35] After fixation with 1.5% paraformaldehyde, cells were immunostained with rabbit anti-Flag Ab or fluorescein isothiocyanate–conjugated mouse anti–c-Myc Ab (Sigma-Aldrich). The cells were then stained with Alexa Fluor 546–conjugated goat anti–rabbit immunoglobulin G secondary Ab (Molecular Probes). Nuclei were counterstained with Hoechst (H33342). Fluorescent images were analyzed on a confocal microscope (FLUOVIEW FV300 scanning laser biological microscope JX70 system; Olympus) equipped with SenSys/0L cold charge-coupled device (CCD) camera (Olympus). The objective lens (an LCPlanFI 60×/1.40 NA oil) was used.

Gel shift assay

Nuclear extracts from transfected 293T cells were incubated with 2 μg of polydeoxyinosinic-deoxycytidylic acid and then with double-stranded

Table 1. Clinical features and genetic findings of the patients with *CEBPA* mutations

Patient no.	Age, y/sex	Diagnosis	N terminal C terminal			Karyotype	Other gene mutation*	Survival (years)
			p30 type	bZIP inframe	Frameshift			
MDS/AML								
142	79/F	AML following MDS	I62fsX160	-	-	46,XY[20/20]	-	1.0
829	70/M	AML following MDS	P51fsX160	-	-	45,XY,der(17;18)(q10;q10)[2/20]/46,XY[18/20]	-	0.4
769	69/M	AML following MDS	-	R297P	-	46,XY[20/20]	*AML1, PTPN11*	1.6
896	77/M	AML following MDS	-	K313del	-	46,XY[20/20]	-	0.6
22	71/M	AML following MDS	-	-	G176fsX317	47,XY,+1,der(1;15)(q10;q10)[20/20]	-	0.8
679	89/M	MDS(RAEB)	-	-	P235fsX318	46,XY[20/20]	-	1.9
806	77/M	AML following MDS	G38fsX107	-	R291fsX313	46,XY[20/20]	-	1.9
Therapy-related AML or MDS								
59	80/F	AML(M4)	L19fsX159	-	-	47,XX,+8,t(9;11)(p22;q23)[20/20]	*AML1*	1.7
158	72/F	AML following MDS	F106fsX154	-	-	46,XX[20/20]	-	1.0
811	76/M	MDS(RAEB)	E59X†	-	-	46,XY[20/20]	-	1.7
1068	66/M	MDS(RAEB)	-	Q305P	-	46,XY[20/20]	-	> 1.5
346	59/M	AML following MDS	-	-	S190fsX320	43,XX,del(5)(q31),-7,-15,-18,-21,+mar [20/20]	*N-RAS*	0.8
577	56/F	AML following MDS	-	-	C213X	46,XX[20/20]	-	2.4
629	89/F	AML following MDS	-	-	L350fsX360	46,XX[20/20]	-	1.2
920	69/F	AML(M5)	-	-	S348fsX422	46,XX,t(11;17)(p15;q21)[20/20]	-	0.2
***De novo* AML(M2)**								
40	68/F	AML(M2)	A111fsX166	S299_L304dup	-	46,XX[20/20]	-	> 10.5
292	75/F	AML(M2)	F33fsX107	R297P	-	46,XX[20/20]	-	> 8.4
662	58/F	AML(M2)	S65fsX167	K313dup	-	46,XX[20/20]	-	> 5.0
888	70/F	AML(M2)	A111fsX166	N321D	-	47,XX,+8[20/20]	-	> 3.8
941	31/F	AML(M2Eo)	T60fsX159	304_323dup	-	46,XX,del(7)(q32)[20/20]	-	> 3.5

RAEB indicates refractory anemia with excess blasts.
*Indicates that no mutation was detected in *AML1*, *N-RAS*, *FLT3*, *PTPN11*, *C-KIT*, and *TP53* genes.
†Homozygous mutation.

CSF3R promoter oligonucleotide labeled with γ^{32}P-adenosine triphosphate. Cold competition and a super-shift reaction were carried out by adding a 40-fold excess of cold CSF3R oligo or 1.5 μg of anti-C/EBP (14AA)X Ab (Santa Cruz Biotechnology), respectively. The resulting complexes were resolved on 4.5% polyacrylamide gel.[44]

Colony assay

Infected mouse bone marrow (BM) mononuclear cells (1×10^4) were plated in methylcellulose medium (StemCell Technologies) supplemented with 50 ng/mL each of interleukin (IL)–3, IL-6, stem cell factor, and granulocyte/macrophage-colony-stimulating factor (GM-CSF; R&D Systems) in the presence of 1 μg/mL puromycin. Colonies were counted after 1-week culture, and single-cell suspensions (10^4 cells) of drug-resistant colonies were subsequently replated.

Mouse BMT

Mouse BMT was performed as described previously.[40] Briefly, BM mononuclear cells were isolated from the femurs and tibias of C57BL/6 (Ly-5.1) donor mice 4 days after intraperitoneal administration of 150 mg/kg 5-fluorouracil. The cells were stimulated with 50 ng/mL of mouse stem cell factor, mouse FLT3 ligand, mouse IL-6, and human thrombopoietin (all cytokines were from R&D Systems). The prestimulated cells were infected for 60 hours with the retroviruses harboring pMYs-C/EBPα-C^m-IG, pMYs-C/EBPα-N^m-IG, pMYs-Myc-tagged C/EBPα-C^m-IG, pMYs-Flag-tagged C/EBPα-N^m-IR, pMYs-Flt3-ITD-IG, pMYs-IG, or pMYs-IR, using 6-well dishes coated with RetroNectin (Takara Bio). Then, $3\text{-}5 \times 10^5$ of the infected BM cells (that had not been sorted after either single or double infection) were injected into sublethally γ-irradiated C57BL/6 (Ly-5.2) recipient mice. Overall survival of transplanted mice were estimated using the Kaplan-Meier method. All animal studies were approved by the Animal Care Committee of the Institute of Medical Science, The University of Tokyo.

Statistical analysis

Statistical significance was calculated using the Student *t* test for independent variables. *P* values $< .05$ were considered statistically significant.

Results

CEBPA mutations in patients with myeloid malignancies

After we performed single-strand conformation polymorphism analysis to screen for *CEBPA* mutations in patients with hematologic disorders, *CEBPA* mutations were identified in 7 of 224 MDS/AML patients, 8 of 71 therapy-related AML or MDS patients, and 5 of 89 de novo AML patients (Table 1). Although the number of the de novo AML patients with *CEBPA* mutations were small, they all carried both an N-terminal mutation and a C-terminal bZIP in-frame mutation on the different alleles as reported previously.[20-26] On the other hand, most MDS/AML or therapy-related AML or MDS patients had single *CEBPA* mutations. As exceptions, we found both an N-terminal mutation and a

C-terminal frame-shift mutation in 1 case of AML after MDS (patient [Pt] #806) and homozygous N-terminal frame-shift mutations in one case of therapy-related MDS/RAEB (Pt #811). Examination of other genes (*RUNX1, N-RAS, FLT3, PTPN11, C-KIT,* and *TP53* gene) in these patients demonstrated that one case of MDS/AML (Pt #769) had both *RUNX1* and *PTPN11* mutations and that patients with therapy-related AML or MDS (Pt #59 or #346) had a mutation of *RUNX1* or of *N-RAS*, respectively. Consistent with recent reports,[22,26] our clinical data showed that overall survival was better in de novo AML patients with double *CEBPA* mutations compared with others with single *CEBPA* mutations (Table 1). These results suggested that double *CEBPA* mutations were able to induce AML, whereas single *CEBPA* mutation would lead to more aggressive AML, in concert with other gene alterations that have not been fully characterized.

The C-terminal but not N-terminal mutations of C/EBPα inhibited G-CSF–induced differentiation of 32Dcl3 cells into mature neutrophils

For further analysis, we chose an N-terminal mutant producing p30 designated as C/EBPα-N^m and a C-terminal b-ZIP in-frame mutant designated as C/EBPα-C^m (Figure 1A). C/EBPα-WT, C/EBPα-N^m, C/EBPα-C^m, C/EBPα-p30, or mock (pMXs-IP) was expressed in Plat-E cells. Expression of p42 protein or p30 protein generated by Myc-tagged C/EBPα-WT and mutants was verified by using anti-Myc Ab as bands corresponding to expected molecular weights (Figure 1B). In addition, we confirmed that N-terminal polypeptide produced by C/EBPα-N^m was detected by anti-C/EBPα Ab recognizing the N-terminal portion of C/EBPα (supplemental Figure 1, available on the *Blood* Web site; see the Supplemental Materials link at the top of the online article). Notably, the expression levels of p30 generated by C/EBPα-N^m were lower than those generated by C/EBPα-p30 (Figure 1B), indicating that deletion of the N-terminal part including the first start codon might increase the expression levels of p30 protein. We then infected 32Dcl3 cells with retroviruses harboring C/EBPα-WT or mutants, and the infected cells were subjected to drug selection. The 32Dcl3 cells expressing detectable levels of C/EBPα-WT were not obtained, presumably due to its strong inhibitory effect on proliferation. Western blot analysis showed that 32Dcl3 cells transduced with C/EBPα-C^m expressed the full length of C/EBPα-C^m at high levels (Figure 1B). C/EBPα-N^m or C/EBPα p30 transduced into 32Dcl3 cells was detected as a band (30 kDa), but the expression level of the former was much lower than that of the latter (Figure 1B). Growth speed was comparable among these transfectants in the presence of IL-3 (Figure 1C). However, the potential of these transfectants to differentiate in response to G-CSF varied; G-CSF treatment induced terminal differentiation of 32Dcl3 cells transduced with mock, as indicated by the appearance of polymorphonucleated neutrophils and up-regulation of CD11b on the surface (Figure 1D-E). G-CSF–induced granulocytic differentiation of 32Dcl3 cells was profoundly inhibited by C/EBPα-C^m, while it was only weakly inhibited by C/EBPα-N^m (Figure 1D-E). The differentiation was also attenuated by C/EBPα-p30, as reported previously.[45] We reasoned that the difference of 32Dcl3 cells expressing C/EBPα-N^m or C/EBPα-p30 in the granulocytic differentiation levels was due to the dissimilar expression levels of a short form of C/EBPα (30 kDa). As for the expression levels of G-CSF-R transcripts, a target of C/EBPα, they were extremely or moderately decreased in 32Dcl3 cells expressing C/EBPα-C^m or C/EBPα-p30, respectively, compared with other transfectants (Figure 1F), implicating G-CSF-R in induction of granulocytic differentiation. However, when human G-CSF-R was transduced into C/EBPα-C^m-expressing 32Dcl3 cells, G-CSF–induced granulocytic differentiation was not completely recovered (supplemental Figure 2). These results indicated that the differentiation block in 32Dcl3 cells expressing C/EBPα-C^m was presumably due to the suppression of C/EBPα activation, but not simply due to the decreased expression of G-CSF-R downstream of C/EBPα.[46]

C/EBPα-C^m or C/EBPα-N^m suppressed the transcriptional activity of C/EBPα-WT by different mechanisms

We next analyzed the transcriptional activation of C/EBPα-WT and mutants in 293T cells using a luciferase construct harboring 2 C/EBPα binding sites. As expected, C/EBPα-WT strongly activated this promoter, while neither C/EBPα-C^m, C/EBPα-N^m, nor C/EBPα-p30 showed any transcriptional activation (Figure 2A). We next examined whether these C/EBPα mutants affected the transcriptional activation of C/EBPα-WT. Although C/EBPα-C^m reduced G-CSF-R expression and inhibited G-CSF–induced myeloid differentiation of 32Dcl3 cells even more efficiently than C/EBPα-N^m (Figure 1D-F), C/EBPα-N^m as well as C/EBPα-p30 but not C/EBPα-C^m decreased promoter activity in the luciferase assay in 293T cells (top panel in Figure 2A), which was in accordance with the data shown by Gombart et al.[20] Expression of C/EBPα WT and mutants in the transfected 293T cells was verified by Western blot analysis (bottom panel in Figure 2A). These results indicated that C/EBPα-C^m and C/EBPα-p30 suppressed expression of G-CSF-R by different mechanisms. Interestingly, transcriptional activation of C/EBPα-WT drastically increased in 293T cells when coexpressed with PU.1, although PU.1 itself did not stimulate the same promoter (top panel in Figure 2B). Notably, this synergistic effect was suppressed by C/EBPα-C^m and weakly by C/EBPα-N^m with low expression levels of p30 protein (top panel in Figure 2B). Expression of C/EBPα and PU.1 was also confirmed by Western blot analysis (bottom panel in Figure 2B). Therefore, we assumed that C/EBPα-C^m was interacting with other transcription factors such as PU.1, thereby suppressing the activation of C/EBPα-WT in hematopoietic cells. We also tested whether the C/EBPα mutants inhibit E2F activity. However, neither C/EBPα-C^m nor C/EBPα-N^m repressed E2F1/DP1-mediated transcription (supplemental Figure 3). In this regard, there was no difference between C/EBPα-C^m and C/EBPα-N^m. We then compared the DNA-binding ability of C/EBPα-WT and mutants by electrophoresis mobility shift assay. As shown in Figure 2C, C/EBPα-WT protein bound to the CSF3R (G-CSF-R) probe, and C/EBPα-p30 protein generated by C/EBPα-N^m less efficiently bound to the same probe. Binding was verified by super-shift of the DNA-protein complex by the anti-C/EBPα Ab. Remarkably, C/EBPα-C^m failed to bind the CSF3R probe (Figure 2C). Next, we examined subcellular localization of C/EBPα-WT and mutants. In line with previous reports, C/EBPα-WT and mutants localized in the nucleus of the interphase cells (Figure 2D). However, it was noteworthy that unlike C/EBPα-WT and C/EBPα-p30, C/EBPα-C^m was not localized on chromosome during the mitotic phase (Figure 2D). It is possible that C/EBPα-C^m without a DNA binding ability is stealing some interacting protein from chromosome. Taken together, these results indicated that C/EBPα-N^m suppressed the transcriptional activation of C/EBPα-WT by its direct binding to the promoter or by its heterodimerization with C/EBPα-WT, while C/EBPα-C^m showed the suppressive effect indirectly, probably through interaction with other transcription factors such as PU.1.

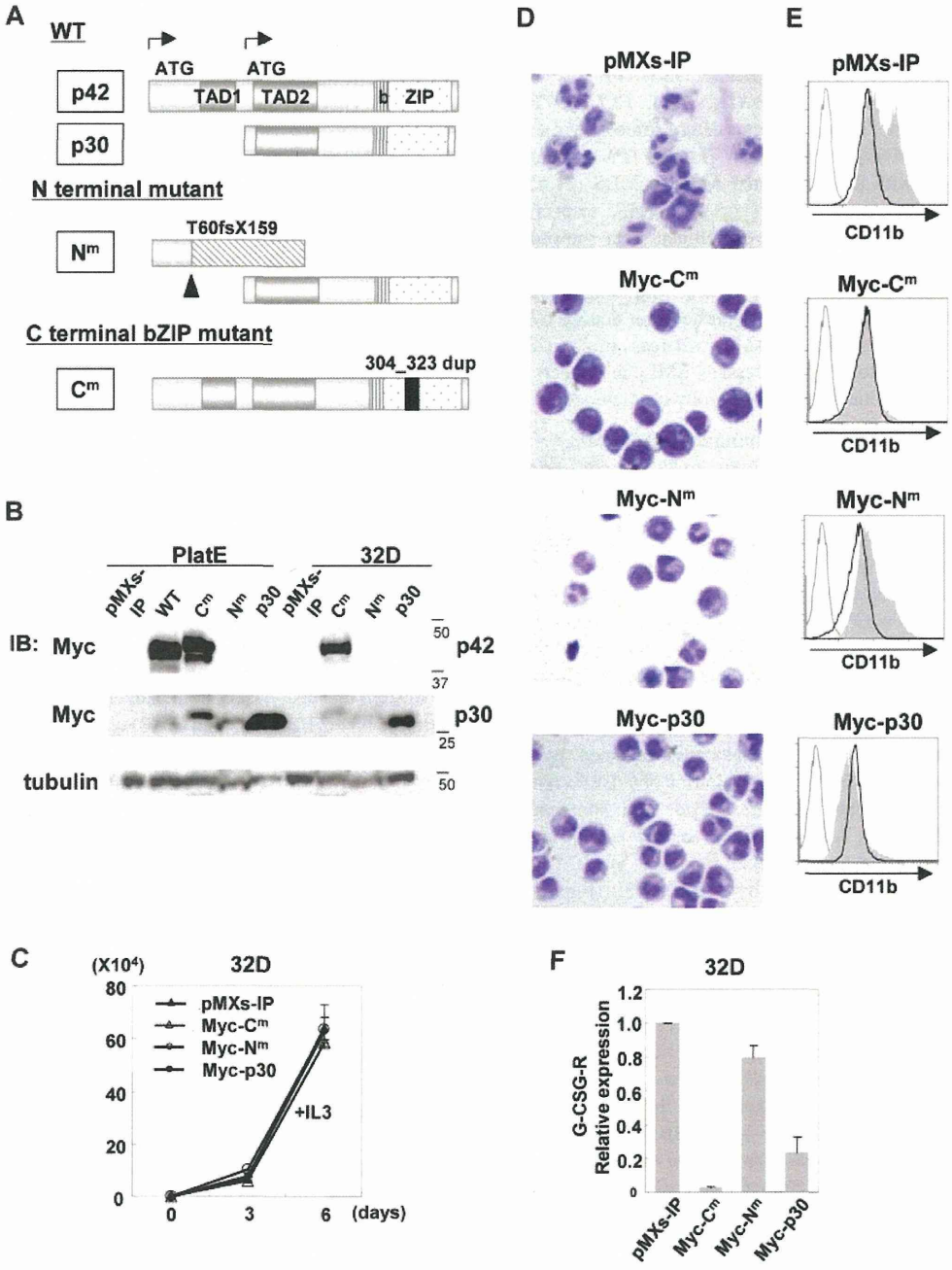

Figure 1. C/EBPα-C^m had the strong ability to block myeloid differentiation. (A) Schematic diagram of C/EBPα-WT (p42 and p30) and mutants, T60fsX159 (C/EBPα-N^m) and 304_323 dup (C/EBPα-C^m). TAD indicates the transcriptional activation domain; bZIP, basic region leucine zipper domain. (B) Expression of C/EBPα-WT and its mutants in Plat-E cells transiently transfected with a Myc-tagged C/EBPα-WT, C/EBPα-C^m, C/EBPα-N^m, or C/EBPα-p30 or an empty vector (pMXs-IP) and expression of C/EBPα mutants in 32Dcl3 cells transduced with Myc-tagged C/EBPα-C^m, C/EBPα-N^m, C/EBPα-p30, or mock (pMXs-IP). Cell lysates were subject to immunoblotting with anti-Myc Ab or anti-tubulin Ab as control. The results shown are representative of 3 independent experiments. (C) The growth of 32Dcl3 cells transduced with Myc-tagged C/EBPα-C^m, C/EBPα-N^m, C/EBPα-p30, or mock (pMXs-IP) in the presence of 1 ng/mL IL-3. All data points correspond to the mean and the standard deviation (SD) of 3 independent experiments. (D-E) 32Dcl3 cells transduced with Myc-tagged C/EBPα-C^m, C/EBPα-N^m, C/EBPα-p30, or mock (pMXs-IP) were cultured in the presence of 50 ng/mL G-CSF for 6 days. (D) Morphology of these cells was assessed by Giemsa staining. Images were obtained with a BX51 microscope and a DP12 camera (Olympus); objective lens, UplanFl (Olympus); original magnification ×40. (E) Surface expression of CD11b in these transfectants after incubation with 1 ng/mL IL-3 (bold histograms) or 50 ng/mL G-CSF (filled histograms) for 6 days was analyzed by flow cytometry. The result of control staining is shown as a thin-lined histogram. Data are representative of 3 independent experiments. (F) Relative expression levels of G-CSF-R in 32Dcl3 cells transduced with Myc-tagged C/EBPα-C^m, C/EBPα-N^m, C/EBPα-p30, or mock (pMXs-IP) were estimated by using real-time PCR. Data are representative of 3 independent experiments.

Retroviral transduction of C/EBPα-C^m, but not C/EBPα-N^m, immortalized BM hematopoietic cells

To determine the effect of C/EBPα-C^m and C/EBPα-N^m on differentiation and proliferation of hematopoietic cells, we performed serial colony-forming assays as described previously.[45] Mouse BM mononuclear cells were transduced with C/EBPα-C^m, C/EBPα-N^m, or C/EBPα-p30. Expression of C/EBPα mutants in the transduced BM cells was verified by Western blot analysis

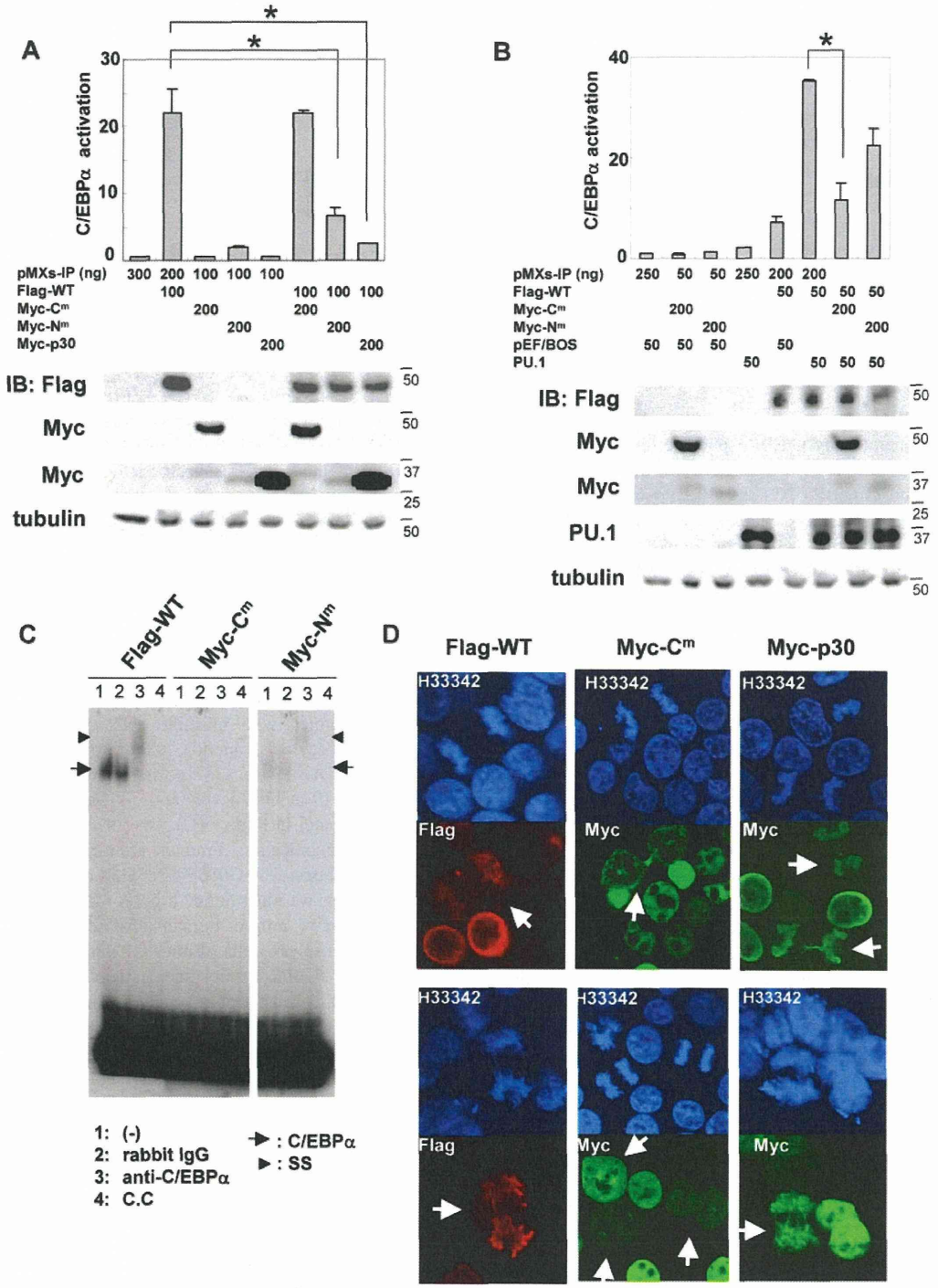

Figure 2. C/EBPα-C^m or C/EBPα-N^m inhibited the transcriptional activation of C/EBPα-WT by different mechanisms. (A-B top) 293T cells were transiently transfected with indicated amounts of expression plasmids (pMXs-Flag-tagged C/EBPα WT-IP, pMXs-Myc-tagged C/EBPα mutants-IP, pMXs-IP, pEF-BOS/PU.1, pEF-BOS) together with 100 ng of the luciferase reporter plasmid p(C/EBP)2TK. The total amount of plasmid for each transfection was adjusted by adding empty plasmids (pMXs-IP or pEF-BOS). Results represented the average values for relative luciferase activity that were normalized using the activity of EF1 vector as an internal control. All transfection groups were normalized with a Renilla luciferase vector as an internal control. All data points correspond to the mean and the standard deviation (SD). Data are representative of 3 independent experiments. Statistically significant differences are shown. *$P < .05$. (Bottom) Expression of C/EBPα-WT, C/EBPα-mutants, or PU.1 in 293T cells transiently transfected as above described. Cell lysates were subject to immunoblotting with anti-Flag Ab, anti-Myc Ab, anti-PU.1 Ab, or anti-tubulin Ab as control. The results shown are representative of 3 independent experiments. (C) DNA binding of C/EBPα-WT and mutants. Electrophoresis mobility shift assay was performed with ^{32}P-labeled oligonucleotides containing the C/EBPα binding site derived from CSF3R promoter and nuclear extracts from 293T cells transiently transfected with pMXs-Flag–tagged C/EBPα WT-IP, pMXs-Myc–tagged C/EBPα-C^m-IP, or pMXs-Myc–tagged C/EBPα-N^m-IP. Data are representative of 3 independent experiments. Lane 1: none (−); lane 2: control rabbit immunoglobulin G was added; lane 3: anti-C/EBPα Ab was added; lane 4: cold competitor (C.C) was added. Ss indicates supershifted bands. (D) 293T cells transiently transfected with pMXs-Flag–tagged C/EBPα-WT-IP, pMXs-Myc-tagged C/EBPα-C^m-IP, or pMXs-Myc–tagged C/EBPα-p30-IP were immunostained with anti-Flag Ab (red) or anti–c-Myc Ab (green) and stained with Hoechst (H33342; blue). Data are representative of 4 independent experiments (total of 15 mitotic cells were examined for each transfectant). Fluorescence images by confocal microscopy were obtained with IX70 (Olympus). Original magnification ×60.

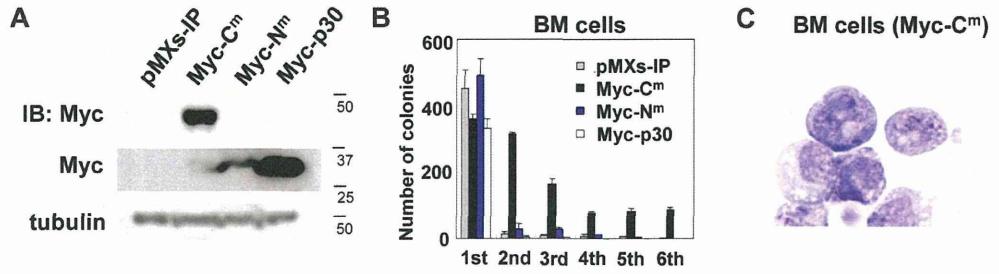

Figure 3. C/EBPα-C^m, but not C/EBPα-N^m, immortalized BM cells. (A) Expression of C/EBPα-C^m, C/EBPα-N^m, or C/EBPα-p30 in BM cells transduced with Myc-tagged C/EBPα-C^m, C/EBPα-N^m, C/EBPα-p30, or mock (pMXs-IP). Cell lysates were subject to immunoblotting with anti-Myc Ab or anti-tubulin Ab as control. The results shown are representative of 3 independent experiments. (B) Colony-forming assay from BM cells transduced with C/EBPα-C^m, C/EBPα-N^m, C/EBPα-p30, or mock (pMXs-IP). Bars represent the number of colonies obtained per 10^4 cells after each round of plating in methylcellulose supplemented with stem cell factor, thrombopoietin, IL-3, and IL-6. Data are representative of 3 independent experiments. All data points correspond to the mean and the standard deviation (SD) of 3 independent experiments. (C) Cytospin preparations of immortalized BM cells transduced with C/EBPα-C^m were stained with Giemsa. Images were obtained with a BX51 microscope and a DP12 camera (Olympus); objective lens, UplanFl (Olympus); original magnification ×100.

(Figure 3A). We also confirmed that the expression levels of p30 protein generated by C/EBPα-p30 are higher than those by C/EBPα-N^m (Figure 3A). Irrespective of different expression levels of p30, most C/EBPα-N^m- and C/EBPα-p30–transduced BM cells did not make secondary colonies after replating (Figure 3B). On the other hand, BM cells expressing C/EBPα-C^m formed colonies after 6 rounds of replating in the presence of cytokine cocktail (Figure 3B). Cytospin preparations of these cells showed blastlike morphologies (Figure 3C). In addition, C/EBPα-C^m–transduced BM cells remained immature and were immortalized in a liquid culture containing IL-3 after several rounds of the replating in semisolid cultures.

Transduction with C/EBPα-C^m into BM cells caused AML in a mouse BMT model

To test whether a single C/EBPα mutant induces hematopoietic abnormality, Ly-5.1 murine BM mononuclear cells, infected with retroviruses harboring C/EBPα-C^m, C/EBPα-N^m, or mock (pMYs-IG), were transplanted into irradiated syngenic Ly-5.2 mice. We confirmed efficient retrovirus infection: 50%-65% of BM cells transduced with C/EBPα-N^m or mock (pMYs-IG) and 35%-50% of BM cells transduced with C/EBPα-C^m were positive for GFP expression before transplantation. Mice receiving transplants of mock (pMYs-IG)–transduced cells (hereafter referred to as mice/pMYs-IG) remained healthy over the observation period (n = 8/8) (Figure 4A). Notably, most of the mice that received transplants of C/EBPα-C^m–transduced cells (hereafter referred to as mice/C^m) developed AML within 4-12 months after transplantation (n = 16/17) (Figure 4A). These morbid mice presented similar phenotypes, characterized by hepatosplenomegaly and pancytopenia (Table 2). BM and spleen were occupied with myeloblasts and myelocytes (Figure 4B). In some cases, leukemic cells displayed morphologic aberrations such as abnormal lobular and ring-shaped nucleus. GFP-positive leukemic cells expressed CD11b and Gr-1 at high levels and c-kit at intermediate to high levels (middle panel in Figure 4C). One of the mice/C^m developed T-cell lymphoma with thymoma (data not shown). We next asked if the integration of retroviruses influenced the outcomes in the BMT model. Southern blot analysis of BM cells of mice/C^m showed a single or several integrations (supplemental Figure 4), and either 1 or 2 integration sites were identified in these samples, based on the inverse PCR method (supplemental Table 1).[47] We found several common integration sites and integrations of the retroviruses in the intron of MN1 in 2 of 15 cases examined (supplemental Table 1). Considering the recent works published by Hasemann et al[48] and by ourselves,[40] retrovirus integration might in part influence the phenotypes of the recipient mice in our BMT models. For example, integration of the retrovirus vector into MN1 may enhance cell growth.[40] However, integration sites do not seem to play major roles in the experiments of this study; C/EBPα-C^m transduction induced AML with similar phenotypes in most cases after a relatively long latency in the BMT model. On the other hand, 5 of 8 mice that received transplants of C/EBPα-N^m–transduced cells (hereafter referred to as mice/N^m) remained healthy during the observation period. Three of 8 mice/N^m developed B-cell acute lymphoblastic leukemia (B-ALL) with hepatosplenomegaly with latencies of 7 to 12 months after transplantation (Figure 4A). BM was occupied with blastlike cells, and the morbid mice exhibited leukocytosis, anemia, and thrombocytopenia (Figure 4B and data not shown). GFP-positive leukemic cells expressed B220 and CD19 at high levels and c-kit at intermediate to high levels (right panel in Figure 4C). One of the mice/N^m developed AML with splenomegaly 13 months after transplantation (data not shown). The reason why C/EBPα-N^m tend to induce B-ALL is not clear. However, we must notice a point that mouse BMT models may not always mimic human diseases.[35,40] Expression of C/EBPα-C^m in spleen cells of mice/C^m with AML or p30 protein generated by C/EBPα-N^m in spleen cells of mice/N^m with B-ALL was confirmed by Western blot analysis (Figure 4D). Collectively, C/EBPα-C^m has a potential to strongly induce AML in a BMT model. Because the latency is relatively long and the leukemic cells seem to be clonal, additional events should have worked with C/EBPα-C^m in inducing leukemia. In addition, the in vivo suppressive effect of C/EBPα-C^m on the activation of endogenous C/EBPα was confirmed by the finding that G-CSF-R expression was down-regulated and c-Myc expression was up-regulated in BM samples of mice/C^m compared with mice/pMYs-IG (Figure 4E-F).

Transduction with both C/EBPα-C^m and C/EBPα-N^m induced more aggressive AML with leucocytosis

To next ask whether the combination of both C/EBPα-C^m and C/EBPα-N^m would induce AML more efficiently, we performed BMT, using murine BM mononuclear cells infected with retroviruses harboring Myc-tagged C/EBPα-C^m-IRES-GFP and Flag-tagged C/EBPα-N^m-IRES-dsRED. BM mononuclear cells expressing both mutants were recognized as GFP- and dsRED-double positive cells, 10%-22% of BM cells before the transplantation. Notably, mice that had received transplants of BM cells expressing both mutants (hereafter referred to as mice/Myc-C^m/Flag-N^m) developed AML with hepatosplenomegaly with shorter latencies